

NATIONAL ADVISORY COMMITTEE FOR AERONAUTICS

# WARTIME REPORT

ORIGINALLY ISSUED

December 1943 as  
Advance Confidential Report 3L23

INVESTIGATION OF FLOW IN AN AXIALLY SYMMETRICAL  
HEATED JET OF AIR

By Stanley Corrsin  
California Institute of Technology



WASHINGTON

NACA WARTIME REPORTS are reprints of papers originally issued to provide rapid distribution of advance research results to an authorized group requiring them for the war effort. They were previously held under a security status but are now unclassified. Some of these reports were not technically edited. All have been reproduced without change in order to expedite general distribution.

NATIONAL ADVISORY COMMITTEE FOR AERONAUTICS

ADVANCE CONFIDENTIAL REPORT

INVESTIGATION OF FLOW IN AN AXIALLY SYMMETRICAL  
HEATED JET OF AIR

By Stanley Corrsin

SUMMARY

The first phase of this investigation was concerned primarily with the determination of a suitable aerodynamic setup. When the final flow arrangement was achieved, attention was turned to the measuring equipment.

In order to permit a thorough investigation of the mechanism of the spread of free turbulence, a new four-wire, two-amplifier hot-wire set was constructed. Automatically recording mean velocity and temperature instruments also were made and were used in the initial stage of the research in the final jet setup. The preliminary runs consisted of measurements of mean velocity and temperature distributions along diameters of several sections normal to the axis of the heated air jet issuing from a convergent-straight nozzle with a mouth diameter of 3 inches. The sections ranged from the nozzle mouth to an axial distance of 12 diameters, or 36 inches. Preliminary measurements also were made of the axial component of turbulence in the center region of each cross section.

The preliminary results displayed serious asymmetry at relatively low axial distances. Since the effect appeared to be due to external disturbances, the change to a smaller jet size was indicated to permit measurements at greater axial distances. All the final measurements were carried out by the author in the jet issuing from a nozzle 1 inch in mouth diameter.

In this 1-inch heated jet, lateral diametrical traverses of mean velocity, temperature, and the axial component of the turbulence were run at several stations between the end of the potential cone and an axial distance of 40 diameters from the mouth. At an axial distance of 20 diameters, measurements also were made of the radial component of the turbulence, of the correlation between axial and radial components of turbulence at the same point, and of the correlation between the axial

turbulent velocities at equal-speed points on opposite sides of the jet axis.

Oscillograms were taken of the axial velocity fluctuations at several points along the jet radius at 20 diameters. These oscillograms together with the correlation measurements indicate that completely turbulent flow exists only in the center region of the jet, forming a turbulent core. It is found that the flow in the extremely low velocity region at the edge is apparently laminar, corresponding to a sort of laminar collar; while between these is an annular "transition" region where the flow fluctuates between the laminar and the turbulent states.

The temperature was found to spread more rapidly than the velocity, as has been recorded in all previously published results.

The diametrical distributions of mean velocity and temperature are compared with the results of three theories for fully developed turbulent flow in a free heated jet with constant density and viscosity. It is found that, in each case, either the velocity or the temperature distribution (depending upon the scale of abscissas) can be made to give a fairly good check between theory and experiment in the turbulent jet core, but never both velocity and temperature simultaneously.

An oscillogram also was taken of the regular fluctuations existing in the region of the jet before the end of the potential cone. This type of fluctuation was first observed in the 3-inch jet by Mr. Thiele in 1940.

## INTRODUCTION

The work done under this contract falls essentially into two parts: The first part was the design and construction of the equipment and the running of preliminary tests on the 3-inch jet, carried out by Mr. Carl Thiele in 1940; the second part, consisting of the measurements in the 1-inch jet and the preparation of this final report, was carried out by the author.

For a complete investigation of the general characteristics of a turbulent flow, some rather complicated

measurements are necessary. Because of this and because of the increasing difficulty in obtaining electrical supplies, it was decided in 1941 that any new equipment needed in the further investigation of the general turbulence problem should be constructed immediately. Accordingly, a very complete hot-wire set was designed and built in the fall of 1941, and was first applied in this research project.

In an approach to the general problem of free turbulence, an investigation of the flow in a free jet is of particular interest. Up to the present time, it has been assumed that the flow in the free jet issuing from a circular orifice into a stationary medium of the same density and viscosity reaches a fully developed condition at about 8 or 10 diameters from the orifice - that is, fully developed in the sense of attaining a configuration which is maintained with similarity downstream. In an axially symmetrical jet it has been found that the "potential cone," in which the velocity is equal to that at the nozzle mouth, has its apex about  $4\frac{1}{2}$  diameters from the mouth, but that the final (dimensionless) velocity profile is not reached until the distance of 8 or 10 diameters previously mentioned.

Ruden (reference 1) and Kuethe (reference 2) have both made measurements in jets with axial symmetry. Ruden measured velocity and temperature distributions out to an axial distance of about 15 diameters in a heated jet; while Kuethe measured detailed velocity distributions and made some turbulence measurements out to 9 diameters in an unheated jet. Both investigators found that similarity of velocity profiles was reached before 10 diameters, which led to the general belief that complete mechanical similarity in a jet was reached there. It was thought, however, that the turbulence distribution in a radial direction might serve as an indication of a fully developed state. Furthermore, it was felt that the limit of 15 diameters, which appeared to be the greatest axial distance included in any previously published results, might be insufficient to give a comprehensive picture of the nature of the flow. The investigation program, therefore, was set up to include complete measurements of at least the axial component of turbulence and sectional traverses out as far as 40 diameters from the nozzle mouth.

All turbulent-jet analyses published up to the present

time are based upon the fundamental assumption that the flow is completely turbulent across the entire width of the jet. The two turbulent jet theories most widely accepted at the present time are Prandtl's momentum transfer theory (reference 3), and the modified vorticity transfer theory of G. I. Taylor (reference 4). In this report there also are included the results of a third method of attack on the general turbulence problem, presented by P. Y. Chou (reference 5). The particular application of this theory to a jet has been made by C. C. Lin, currently at the GALCIT. This approach is equivalent to the assumptions suggested by T. von Kármán (reference 6). The application of the momentum transfer assumptions to this problem was carried out by W. Tollmien (reference 7), the calculation of the modified vorticity transfer principle applied to a jet was made by Tomotika (reference 8), and the results of the two theories were summarized by L. Howarth (reference 9). Also, the problem of the velocity distribution in the annular region around the potential cone of an axially symmetrical jet has been solved on the basis of the momentum transfer assumptions by A. M. Kueths. Shortage of time has precluded the comparison of the 3-inch jet measurements with Kueths's solution.

A comparison of the distributions of mean velocity and temperature in a free jet the initial temperature of which is slightly different from that of the receiving medium presents an excellent opportunity for comparison of the rates of diffusion of the two quantities, momentum and heat, without introducing the complexity of variable viscosity and density.

This investigation, conducted at the California Institute of Technology, was sponsored by, and conducted with financial assistance from, the National Advisory Committee for Aeronautics. The work was carried out under the general supervision of Dr. T. von Kármán and Dr. C. B. Millikan, whose interest and advice are gratefully acknowledged. Particular thanks are due to Mr. Carl Thiele for his splendid job of designing and constructing the equipment and getting the research under way and to Dr. Hans Liepmann for his invaluable counsel and advice throughout the research. Theoretical discussions on many occasions with Mr. C. C. Lin were also of great assistance.

## SYMBOLS

- d diameter of nozzle mouth
- x axial distance from mouth
- r radial distance from jet axis
- U axial component of mean velocity,\*
- V radial component of mean velocity
- W tangential (rotational) component of mean velocity
- $U_R = \sqrt{U^2 + V^2}$
- $U_m$  = maximum value of U at a section (i.e., on the axis)
- $U_0$  maximum value of U in the jet (in potential cone)
- $r_0$  the value r at any section for which  $U = \frac{1}{2} U_m$
- u axial component of instantaneous velocity fluctuation
- v radial component of instantaneous velocity fluctuation
- w tangential component of instantaneous velocity fluctuation
- $u' = \sqrt{u^2}$
- $v' = \sqrt{v^2}$
- $w' = \sqrt{w^2}$
- $\frac{u'}{U}, \frac{v'}{U}, \frac{w'}{U}$  turbulence levels
- P pressure
- $\rho$  air density

---

\*Mean values of velocity and temperature referred to in symbols are time means.

- $\mu$  air viscosity coefficient
- $\nu = \frac{\mu}{\rho}$  air kinematic viscosity
- $\tau$  shear
- $T$  mean temperature, measured above room temperature
- $T_m$  maximum value of mean temperature at a section  
(i. e., on the axis)
- $T_o$  maximum value of mean temperature in the jet (at the  
mouth)
- $t$  instantaneous temperature fluctuation
- $t' = \sqrt{t^2}$
- $l$  "mixing length" in momentum transfer theory
- $\lambda$  "micro-scale" of turbulence
- $\overline{AB}$  correlation between any two fluctuating quantities,  
A and B
- $R_{uv} = \frac{\overline{u'v'}}{u'v'}$  correlation coefficient
- $R_u = \frac{u_1 u_2}{u^2}$  correlation coefficient
- $E_T$  total kinetic energy crossing a section of the jet  
in unit time
- $E_M$  kinetic energy of mean flow crossing section in  
unit time
- $E'$  turbulent kinetic energy crossing section in unit  
time

## I. PRELIMINARY MEASUREMENTS ON A JET 3 INCHES IN DIAMETER

### EQUIPMENT AND TESTING PROCEDURE

#### Aerodynamic Setup

Figure 1 is a schematic diagram of the wind-tunnel and installed jet units. The four-blade steel propeller is driven by a three-phase induction motor rated at 15 horsepower and run from a variable frequency generator. In all this work, the unit was run at only a small fraction of rated power.

The 6½-foot square "pressure box" was adapted from the former GALCIT calibration tunnel. The air is heated by means of 16 Calrod heating units mounted in the primary contraction (fig. 2), and there are two screens mounted between the heaters and the final jet contraction, which was a spun aluminum convergent nozzle. In an effort to obtain a uniform temperature distribution across the mouth of the nozzle, part of the heated air was ducted along the outside of the large circular pipe leading to the nozzle, so that this pipe and the beginning of the nozzle contraction were immersed in heated air. That this scheme was not completely successful can be seen from the temperature distribution measured at the mouth. It did represent, however, a distinct improvement over the wooden nozzle first tried. Possibly this inaccuracy in one of the temperature boundary conditions had an effect upon the temperature profiles in the region of the jet upstream from the end of the potential cone, as will be discussed later.

All tests on the 3-inch jet were run at a mouth velocity of 20.5 meters per second and a maximum temperature difference of about 13° C.

The platinum hot wires used to measure  $u'$  were etched Wollaston, 0.00025 inch in diameter and approximately 2 millimeters in length. Mean velocity, was measured with a small total head tube, and temperature was measured with a small copper-constantan thermocouple.

The amplifier output for turbulence readings was put through a thermocouple into a critically damped wall galvanometer with a 3-second period and a full scale deflection of approximately 20 centimeters.

Both mean speed and temperature were photographically recorded by means of an automatic-traversing arrangement. The total-head pressure line was run into a small copper bellows which tilted a mirror, thereby deflecting a narrow light beam upon a uniformly moving sheet of sensitized paper.

The recording of temperature on the sensitized paper utilized directly the light beam reflected from the mirror of the wall galvanometer.

The traversing was accomplished by means of a screw-driven carriage running horizontally along a steel track. The screw was rotated by a reversible electric motor and, during the photographically recorded runs, the sensitized paper was mechanically connected to the hot-wire carriage so that the abscissas of the recorded curves would be exactly equal to the true lateral distances. Figures 4 and 5 show an over-all view of the traversing unit and a close-up of the carriage and motor. Photographs are of the 1-inch jet installation, which was identical with that for the 3-inch jet unit, except for the wall in the plane of the nozzle mouth in these pictures.

#### Measuring Equipment and Procedure

This new hot-wire set (photographed in fig. 6) consists of the following elements:

1. Four hot-wire heating circuits and potentiometer
2. One bridge circuit which can be used with any of the four heating circuits
3. Two compensated amplifiers with very nearly the same phase shift and gain characteristics
4. One amplifier in which the outputs of the other two amplifiers can be added

With this instrument the following flow properties can be measured:

1. Mean speed,  $U$
2. The three principal turbulence components,

$$\frac{u'}{U}, \frac{v'}{U}, \frac{w'}{U}$$

3. The correlations at a point,  $\overline{uv}$  and  $\overline{uw}$
4. The correlations between turbulent velocity components at two points, in flows with or without a gradient in the mean velocity

The bridge circuit is so arranged that the hot-wire "time constant" can be determined by superimposing equal alternating-current voltages at two frequencies upon the balanced direct-current bridge circuit.

The gain of each amplifier is constant to within  $\pm 3$  percent over a frequency range from 5 to 9000 cycles per second.

#### RESULTS OF THE PRELIMINARY MEASUREMENTS

The measured results are plotted in figures 8 to 16. Figure 8 shows the distribution of mean velocity, mean temperature, and turbulence along the axis of the jet. The velocity is plotted both uncorrected and approximately corrected for the effect of turbulence upon the total head tube readings. Assuming constant static pressure throughout the jet, the average pressure at the mouth of tube in a turbulent flow is:

$$P = \frac{\rho}{2} \overline{(U + u)^2}^*$$

where  $U$  is the axial mean velocity and  $u$  is the instantaneous axial velocity fluctuation. Therefore,

$$P = \frac{\rho}{2} (U^2 + \overline{u^2})$$

since

$$\overline{Uu} = 0;$$

and the dynamic pressure corresponding to the mean velocity is

$$\frac{\rho}{2} U^2 = \frac{P}{1 + \frac{\overline{u^2}}{U^2}}$$

\*Neglecting the effect of lateral fluctuations.

Figures 9 to 16 give the measured mean velocity and temperature distributions across sections normal to the jet axis. All of these velocity and temperature distributions were continuously recorded photographically, and the plotted results are curves faired through the photographic data. Since this continuous recording method tends to give instantaneous fluctuations in the quantity being measured (unless considerable overdamping is employed), the scatter of the photographic curves is appreciably greater than that of point-by-point measurements which involve a process of mental time-averaging in the recording of the observed data.

The distributions of turbulence level along the axis and in sections normal to it are also given in these figures. Unfortunately, since the transverse measurements have been made in only the central part of the jet, a complete picture cannot be gotten from them.

## DISCUSSION OF RESULTS

### Velocity and Temperature

Asymmetry in the velocity profiles becomes appreciable at an axial distance of about 4 diameters, and appears even sooner in the temperature curves. The nature of the velocity asymmetry, a high region on the left side of the axis for  $\frac{U}{U_m} < 0.4$ , seems to indicate that the flow condition actually existed, due perhaps to external disturbance or to misalignment of the nozzle relative to its circular duct. On the other hand, the temperature asymmetry consists of an apparent change in the zero-ordinate level between opposite sides of the jet, and it appears more likely that this is due to the method of measurement than that it is representative of a true condition of the jet.

One of the theoretical boundary conditions for this jet problem is not precisely satisfied: The temperature profile at the jet mouth deviates appreciably from a rectangular shape in spite of the ducting system for heating the walls of the channel leading to the nozzle. Even so, this temperature profile represented a considerable improvement over that existing in the jet emerging from the

wooden convergent nozzle with which these experiments were first tried.

It has not been determined whether the nature of the deviation from this particular boundary condition has any appreciable effect on the difference in the relation of the velocity and temperature profiles in the two regions of the jet separated by the section at an axial distance of about 7 diameters from the mouth. For  $x < 7d$ , the curve of  $\frac{T}{T_m}$  is lower than  $\frac{U}{U_m}$  in the central part of the jet, while for  $x \geq 7d$  the temperature is everywhere higher. It is possible that the existence of a definite temperature gradient in the main body of the jet at  $x = 0$ , where there is no corresponding velocity gradient, has accentuated the condition.

It seems probable, however, that this change in relative shapes of the velocity and temperature profiles is a true characteristic of a heated jet. In the region upstream of the potential cone the flow may be approximated by the two-dimensional case of the single mixing region between a semi-infinite moving body of heated air and a semi-infinite body of stationary cooler air. In this case it seems evident that, if the effective heat-transfer coefficient is assumed greater than the effective shear coefficient, the dimensionless plots of temperature and velocity across a section normal to the flow (i. e., curves of  $U/U_m$  and  $T/T_m$  against the same abscissa  $r/r_0$ ) will show temperature lower than velocity in the region of higher values of the two variables; conversely, they will show temperature higher than velocity in the region of lower values. For the fully developed jet with axial symmetry it is obvious that the same assumption of heat-transfer coefficient greater than shear coefficient leads to dimensionless temperature profiles everywhere higher than the corresponding velocity profiles.

It should also be noted that these velocity and temperature profiles check the measurements of Ruden fairly well.

### Turbulence

The principal item of interest connected with the turbulence measurements is the extremely rapid spread of

turbulence into the potential cone. It will be noted that the turbulence level on the jet axis begins to rise at an axial distance of only 1 diameter from the nozzle mouth; while the velocity defect does not reach the axis until about  $4\frac{1}{2}$  diameters. This result was observed by Kuethe and has been recorded in the 1-inch jet described later. Its significance with respect to open-throat wind tunnels is apparent.

The quantity  $u'/U$  loses some of its usefulness for high values; so  $u'/U_m$  has also been plotted for each section. The full benefit of plotting either  $u'/U_m$  or  $u'/U_0$  will become evident in the 1-inch jet where turbulence has been measured out to the edge of the jet.

## II. FINAL MEASUREMENTS ON A JET 1-INCH IN DIAMETER

### EQUIPMENT

The experimental apparatus employed in this part of the work is basically the same as that used in the preliminary tests, with the following modifications:

1. A 1-inch spun-aluminum convergent nozzle was substituted for the 3-inch nozzle. The internal flow-arrangement was the same.
2. A wall was set up in the plane of the jet mouth, perpendicular to the axis, in order to reproduce more precisely the boundary conditions assumed in the theories. A check run was made without the wall in position, and although no appreciable difference was found in the flow characteristics in the "fully developed" region of the jet, it was decided to run with the wall in position.
3. No photographic-recording technique was used for any of the quantitative measurements, since it was thought that some of the asymmetry in the 3-inch jet measurements might have been due to lag or permanent set in the moving parts of the recording system.
4. Mean speed was measured with a single hot wire instead of a total head tube. One check run was made with a total head tube, and the agreement was satisfactory.

The mean velocity measured by the hot wire was  $\sqrt{U^2 + V^2}$  rather than simply  $U$ . Therefore the experimental results have been labeled accordingly, with the symbol  $U_R$  to signify  $\sqrt{U^2 + V^2}$ . Over all but the edge of the jet  $U_R \doteq U$ , and in the comparison between theory and experimental results,  $U$  (theoretical) is compared with  $U_R$  (experimental). As will be pointed out later, the large discrepancy between experiment and the most satisfactory theory (fig. 30) at the edge of the jet is not due to this comparison of different velocity components.

It should also be remarked that the turbulence component measured by the single hot wire is the component in the direction of  $U_R$ . However, it is everywhere written merely as  $u'$ , since in the turbulent core of the jet the measured component of turbulence is probably equal to the true axial component ( $u'$ ) within the limits of accuracy of the measurements.

The lateral turbulence level is written as  $v'/U_R$  although the  $v$ -meter was always set parallel to the jet axis. However, tests showed that the effect of small deviations in alinement of the instrument from the mean flow direction upon the output was negligible relative to experimental scatter.

5. The lateral component of turbulence and the turbulent correlation  $uv$ , were measured with a biplane X-type meter composed of two platinum wires, each set at an angle of about  $45^\circ$  to the mean flow, and therefore perpendicular to each other. The wires were etched Wollaston, 0.00025 inch in diameter and approximately 4 millimeters in length.

6. A Dumont oscilloscope with 5-inch photographic-type tube and a General Radio high-speed camera were used to record the oscillograms.

7. The scale of  $u'$  turbulence on the jet axis was measured by mounting a second hot-wire carriage on the steel traversing track.

All runs were made at a nozzle velocity of 10 meters per second, and a maximum temperature difference of about  $10^\circ$  C. In order to check the assumption that this temperature difference has no appreciable effect upon the hydro-

dy

dynamic jet characteristics, one traverse was repeated without the addition of heat. The  $U_R/U_m$  and  $u'/U_R$  curves for the two cases checked within the experimental scatter.

Inclination of the jet axis due to free convection was negligible.

### TESTS AND GENERAL PROCEDURE

1. Mean velocity,  $U_R$ : measured with a single hot wire by either constant current or constant resistance method
2. Mean temperature,  $T$ : measured with a small copper-constantan thermocouple across a wall galvanometer
3. Axial turbulence,  $u'$ : measured with a single hot wire in the conventional manner
4. Radial turbulence,  $v'$ : measured with a biplane X-type meter composed of two hot wires the outputs of which are subtracted before being put into the amplifier
5. Double correlation at a point (turbulent shear),  $uv$ : measured with the same meter as  $v'$ . The outputs of the two wires are put through the amplifier separately, and the correlation is computed from these results.
6. Double correlation of axial turbulence at two equal-velocity points on opposite sides of the axis,  $u_1u_2$ : measured with two single hot wires. In order to get a measure of the scale of turbulence, the  $u_1u_2$  was measured as a function of the distance between the wires.
7. Oscillograms of the  $u$ -fluctuations were made, using the single hot wire. The amplifier output was photographed from the screen of an oscilloscope the sweep of which had been cut out. The film motion supplied the continuous sweep.

## RESULTS

Unless specifically described otherwise, all quantities plotted in this report are uncorrected for the effects of turbulence upon the measuring instruments. The nature of these corrections will be discussed later.

### Mean Velocity and Temperature

The measured velocity and temperature distributions along the jet axis and at each station are included in figures 17 and 22. As has been found by Ruden, the temperature spreads at a greater angle than the velocity in the region of  $x$  greater than 8 or 10 diameters. It will be noted also that at 5 diameters, the temperature distribution is narrower than the velocity in the center part of the jet, as recorded and discussed in the first part of the report. No detailed measurements were made in the 1-inch jet for  $x$  less than 5 diameters, but the temperature distribution at the nozzle mouth was checked as being of the same nature as that in the 3-inch jet.

The axial distributions show a crossing, or at least a coincidence, of the velocity and temperature curves at large distances from the nozzle, in spite of the fact that the initial drop-off occurs much sooner for the temperature than for the velocity.

### Turbulence

a) Turbulence level.— The measured local turbulence level  $u'/U_R$  as well as the values of  $u'/U_m$  computed from  $u'/U_R$  and the faired velocity profile, are included in figures 18 to 22. Probably the quantity  $u'/U_R$  loses its significance in regions of extremely low velocity like the edge of the jet. A better comparison of the turbulence distributions at successive stations can be gained from figure 23 where  $u'/U_0$  is plotted against the radius. This clearly shows the radial spread of the fluctuating energy (really, the square root of the energy) as the flow travels in the axial direction.

The only measurement of the radial turbulence component  $v'$  is compared in figure 24 with the  $u'$  at the same station.

b) Correlation between velocity components at the same point.— The correlation and the correlation coefficient are given in figure 25. The coefficient is defined by

$$R_{uv} = \frac{\overline{uv}}{u'v'}$$

the turbulent shear is, of course,

$$\tau = -\rho \overline{uv}$$

and will be discussed in the next section.

The tremendous scatter in  $R_{uv}$  in the outer annulus of the jet, as well as the sharp decrease in both  $R_{uv}$  and  $\overline{uv}$  toward this region, seem to indicate a deviation from the true turbulent state, a hypothesis which receives especial support from the oscillograms of the velocity fluctuations.

c) Correlation between velocity components at different points.— Figure 26 is the one measured distribution of  $R_u$  between points symmetrical about the jet axis. This correlation coefficient is defined by

$$R_u = \frac{\overline{u_1 u_2}}{u^2}$$

An important result shown by this curve is that there is no whipping of the jet as a whole; whipping could result from a general instability of the system. If such a condition existed, the correlation would not go to zero with increasing  $r$ , but would increase negatively.

d) Oscillograms.— The series of oscillograms in figure 27 indicates a definite deviation from the fully turbulent regime toward the edge of the jet. A completely turbulent core exists out to approximately  $r_0$ , the radius at which the mean velocity is one-half the maximum mean velocity at the section, which is, of course, on the jet axis.

Figure 28 shows the type of regular fluctuations first observed in a 3-inch jet by Thiele in 1940. These are

oscillograms of the  $u$ -fluctuations in the 1-inch jet at an axial distance of 2 diameters. The bottom part is a 200 cycle-per-second timing wave, which applies to both figures 27 and 28; figure 28a was recorded on the axis in the potential cone and figure 28b was recorded at a radius equal to the radius of the nozzle mouth. This is approximately the inner edge of the free boundary layer. The layer is evidently turbulent, or the regular waves would continue through it.

## THEORETICAL ANALYSES

### Velocity

For a free jet of this type the usual turbulent boundary layer assumptions are applied to the general Navier-Stokes equation. The simplified equation must be solved with the boundary conditions  $V = 0$  and

$\frac{\partial U}{\partial r} = 0$  at  $r = 0$  (on the axis). Also the velocities

and their derivatives must vanish as  $r$  becomes infinite. Since the axial pressure gradient is neglected, the rate of flow of axial momentum across all sections is the same:

$$2\pi \rho \int_0^{\infty} U^2 r dr = \text{constant}$$

Since viscosity is neglected,

$$\tau = -\rho \overline{uv}$$

a) Momentum transfer theory.— The assumption that momentum is the transportable quantity with a mechanism analogous to the kinetic theory of gases leads to

$$\tau = -\rho \overline{lv} \frac{\partial U}{\partial r}$$

which gives the equation of motion:

$$U \frac{\partial U}{\partial x} + v \frac{\partial U}{\partial r} = -\frac{1}{r} \frac{\partial}{\partial r} \left( \overline{lv} r \frac{\partial U}{\partial r} \right)$$

Prandtl further suggested the assumption of  $v = l \frac{\partial U}{\partial r}$  or, since  $\frac{\partial U}{\partial r}$  is intrinsically negative in an axially symmetrical jet,  $v = -l \left[ \frac{\partial U}{\partial r} \right]$ . This leads to  $\tau = \rho l^2 \left[ \frac{\partial U}{\partial r} \right] \left( \frac{\partial U}{\partial r} \right)$ , and the equation of motion may be written

$$U \frac{\partial U}{\partial x} + v \frac{\partial U}{\partial r} = \frac{1}{r} \frac{\partial}{\partial r} \left[ l^2 r \left[ \frac{\partial U}{\partial r} \right] \left( \frac{\partial U}{\partial r} \right) \right],$$

or

$$U \frac{\partial U}{\partial x} + v \frac{\partial U}{\partial r} = - \frac{1}{r} \frac{\partial}{\partial r} \left[ l^2 r \left( \frac{\partial U}{\partial r} \right)^2 \right]$$

Tollmien assumes similarity at different sections of the jet and assumes that  $l$  is constant across any section and proportional to the radii  $r_0$  of the sections. Having found experimentally that  $r_0 \sim x$ , he assumes  $l = cx$ .

b) Modified vorticity transfer theory.— Taylor assumes that vorticity is the transportable quantity and is carried unchanged from one layer of fluid to another. This, with the assumption of isotropy of turbulence, yields the equation of motion

$$U \frac{\partial U}{\partial x} + v \frac{\partial U}{\partial r} = \overline{lv} \left( \frac{\partial^2 U}{\partial r^2} + \frac{1}{r} \frac{\partial U}{\partial r} \right)$$

Assuming with Prandtl that  $\overline{lv} = l^2 \left[ \frac{\partial U}{\partial r} \right]$ , Howarth and Tomotika have

$$U \frac{\partial U}{\partial x} + v \frac{\partial U}{\partial r} = -l^2 \frac{\partial U}{\partial r} \left( \frac{\partial^2 U}{\partial r^2} + \frac{1}{r} \frac{\partial U}{\partial r} \right)$$

and they also assume  $l = cx$ .

c) A third approach to the calculation of the velocities in turbulent flow was presented by P. Y. Chou. The equations are obtained by constructing correlation functions from the equations of turbulent fluctuations.

In the application of this theory to the jet, Lin has employed, in addition to the boundary layer approximations:

1. The assumption of mechanical similarity of mean quantities extended to include all the double (and triple) correlations
2. Certain considerations based upon similarity of fluctuations, and the microscale of turbulence
3. The assumption that the triple correlations of the turbulent fluctuation which vanish at the center of the jet are negligible throughout the jet

These assumptions result in an expression for the shear which is identical to the form suggested by Von Kármán in 1937:

$$\tau = \frac{\overline{v^2} \lambda^2}{\omega} \frac{\partial U}{\partial r}$$

In addition, Lin assumes

4. That  $\frac{\overline{v^2}}{2}$  and  $\lambda$  are constant. This final assumption amounts to a constant shear coefficient,\* and the form of the solution is the same as that for a laminar jet:

\*Since the writing of this report, copies of two new theoretical papers on the problem of free turbulence have been received. Both authors advocate the assumption of a constant shear coefficient for the calculation of the flow in a free jet. The papers are:

Prandtl, L.: Bemerkung zur Theorie der freien Turbulenz. Z.f.a.M.M., vol. 22, Oct. 1942.

Görtler, H.: Berechnung von Aufgaben der freien Turbulenz auf Grund eines neuen Näherungsansatzes.

$$\frac{U}{U_m} = \frac{1}{\left(1 + \frac{r^2}{4}\right)^2}$$

where

$$\xi = \frac{r}{x}$$

Temperature

With the usual boundary layer approximations, the equation for the temperature  $T$  is

$$U \frac{\partial T}{\partial x} + v \frac{\partial T}{\partial r} = \frac{1}{r} \frac{\partial}{\partial r} \left( \overline{v} r \frac{\partial T}{\partial r} \right)$$

The same general boundary conditions apply to the temperature as were applied to velocity.

a) Momentum transfer theory.— Since the above equation in  $T$  is the same as the equation of motion (in  $U$ ) corresponding to the momentum transfer theory, it follows that the temperature distribution is the same as the velocity distribution.

b) Modified vorticity transfer theory.— The previously obtained solutions for  $U$  and  $V$  are put into the temperature equation, along with the assumption that

$$\overline{v} = -cx^2 \frac{\partial U}{\partial r}$$

as before.

This leads to a solution for  $T/T_m$  as an exponential function which converges much more rapidly than the velocity  $U/U_m$ .

c) In solving for the temperature distribution, Lin uses a constant coefficient of thermal diffusion, analogous to the use of a constant shear coefficient. This leads to a power law relationship between the velocity and temperature distribution, which is written

$$\frac{T}{T_m} = \left( \frac{U}{U_m} \right)^{1/\epsilon_a}$$

where  $\epsilon_a$  is not given by the theory but must be determined experimentally.

## DISCUSSION OF RESULTS

### The Nature of the Flow

Figure 27 is a series of oscillograms of the axial velocity fluctuations at various radial positions on a section 20 diameters from the nozzle mouth. This series shows that the flow in a "turbulent jet" is fully turbulent only out to approximately  $r = r_0$ . For  $r > r_0$ , there exists first an annular "transition region" in which the flow alternates between the turbulent and the laminar regimes. The fraction of the total time during which the turbulent state prevails decreases as the radial distance is increased. Then, near the edge of the jet and extending to zero velocity is what might be termed the annular "laminar collar." Of course, this laminar collar differs from the usual concept of a laminar boundary layer or a laminar sublayer in a turbulent boundary layer next to a wall; the difference is that there exists an appreciable radial ( $V$ ) component in the mean velocity. The disappearance, however, of uv-correlation toward the edge of the jet can be taken as a clear indication that the momentum transfer here is essentially laminar.

The cause of the deterioration of the turbulent flow toward the edge of the jet is not immediately apparent, since there is no solid wall to damp out the  $v$ -fluctuations as in the conventional turbulent boundary layer.

The similarity between this entire flow condition and the history in the mean flow direction of the flow in the boundary layer along a wall is striking. The principal difference is that the sequence of flow regimes extends in a direction perpendicular to the mean flow, while in the latter case it extends in the mean flow direction. The oscillograms of the jet-transition region are identical with some of the oscillograms of the transition from a laminar to a turbulent boundary layer.

A more significant aspect of the verification of this flow pattern in the turbulent jet is that this may present an insight into the nature of the flow in a fully developed turbulent boundary layer next to a solid wall. It is well known that a thin laminar sublayer exists immediately adjacent to the solid boundary, and that there is no sharp

point of demarcation, but a narrow region of transition. The flow in this region is probably of the same nature as the flow in the annular transition region of the turbulent jet.

It will be noted that the general location of the transition region in the jet is more or less the same as the location of the maximums of the  $u'/U_R$  curves at all sections (see figs. 18 to 22). This may mean that a part of the "turbulence" is due not to the usual turbulent velocity fluctuations, but to actual differences in the local mean velocity at a point, as the flow oscillates between the turbulent and the laminar states. This explanation was first given by Liepmann in connection with the studies reported in reference 10 to explain the high apparent turbulence level in the transition region of a boundary layer adjacent to a solid wall. It should, however, be recorded that no definite one-sided turbulent bursts on the oscillogram were seen in the case of the jet.

#### Comparison between Theory and Experiment

a) Velocity.- On figures 29, 30, and 31 are plotted the results of the three theories briefly discussed and the experimentally observed points. For purposes of comparison, the theories and experiment have all been matched at  $r = r_0$ . This seems to be an especially suitable method in view of the fact that this radius is approximately the boundary of the completely turbulent jet core.

In inspecting these figures, it must be remembered that the experimental points have not been corrected for the effect of turbulence upon the hot wire. This correction would appreciably decrease the measured velocity everywhere but near the axis. Qualitatively, such a correction, followed by proper refitting of the experimental points at  $r = r_0$ , would primarily widen the profile peak. Since the problem of correcting hot-wire measurements for the effect of very high turbulence levels ( $u^2/U$  above about 20 percent) is still under consideration at the GALCIT, the results are presented as observed and without correction. The question of turbulence corrections is taken up briefly in appendix II.

It should be mentioned also that the mean speeds at stations 10, 20, and 40 were measured by the constant-current method. In this method, the values at extremely low speeds are too high because of convection cooling, when sufficient current is used to give reasonable sensitivity at the higher speeds. The constant-resistance (and, therefore, constant-sensitivity) method is much more satisfactory when a wide velocity range is to be covered, and was employed at stations 5 and 30. The observations by the two methods diverge perceptibly only at the extreme edge of the jet. In figure 30 the scatter everywhere but at the extreme edges is ordinary experimental scatter.

As mentioned before, similarity in the velocity profile is reached at about  $x = 10$  diameters.

Since the three theoretical analyses assume a turbulent state across the full width of the jet, the degree of agreement between theory and experiment in the region for  $r > r_0$  is evidently of secondary importance. Inspection of the (theoretically) significant region of  $r < r_0$  indicates a satisfactory check between the observed points and the curve based upon a constant shear coefficient. It is obvious that the large discrepancy in the outer part of the jet between experiment and constant shear coefficient theory cannot be due to the method of velocity measurement (hot-wire measures  $U_R$  instead of  $U$ ); correcting the experimental points to be  $U$  instead of  $U_R$  would increase the discrepancy.

The physical requirements of constant flux of momentum across all sections of the jet plus the usual assumption of velocity-profile similarity lead to the requirement of a hyperbolic decrease in the mean speed along the jet axis. A plot of the axial velocity distribution on logarithmic cross-section paper (fig. 35) shows that the decrease approximates a nearly hyperbolic power law from 10 to 30 diameters, but deviates markedly at greater distances. This deviation may indicate either that the velocity decrease does not follow a simple power law or that external disturbances have begun to be felt. A check run of the axial velocity distribution for  $U_0$  more than twice as large as used in all these measurements gave an identical deviation from the hyperbolic distribution. From the experimental setup it appears unlikely that external

disturbances would be felt before  $x = 50$  diameters. If, then, it is assumed that external effects are negligible, this deviation seems to deny the existence of exact similarity, since the constant flux of momentum is a simple physical requirement. The only remaining possibility is that the axial pressure gradient cannot be neglected.

The similarity property, however, of the jet as represented by a linear increase in the width of the velocity profiles with downstream distance is well checked out to  $x = 40$  diameters in figure 36. Surprisingly, the line passes very nearly through the nozzle mouth when extrapolated to zero jet width.

All the theoretical analyses assume mixing length increasing linearly with axial distance:  $l = cx$ . A calculation of  $c$  at  $x = 20$  diameters, based on the momentum transfer theory leads to  $c = 0.0166$ . Tollmien gives a value of 0.0158.

b) Temperature.— Since Lin's analysis does not explicitly give the temperature profile as a function of the velocity profile, but leaves one constant to be determined by experiment, only the results of the other two theories have been plotted in figures 32, 33, and 34 for comparison with the experimental results.

In spite of the considerable scatter, it is evident that theoretical and experimental temperature distributions do not agree if the velocity distributions are matched at  $r = r_0$ . If, on the other hand, the temperatures were fitted at the radius where  $T = 1/2 T_m$ , then the experimental and theoretical velocity profiles would exhibit a wide divergence; while the temperatures would check reasonably well.

Since there is no method of determining which fitting procedure is more nearly correct, the only permissible conclusion is that none of the existing theories gives a satisfactory quantitative relationship between the spread of velocity and the spread of temperature in a turbulent heated jet.

It would seem that a better understanding of the basic relation between the mechanisms of the diffusion of velocity and temperature could be gotten by measurements of the temperature fluctuation ( $t'$ , say, and

perhaps  $\overline{t_1 t_2}$  correlations) and by the comparison of these measurements with the corresponding kinematic quantities.

It should be noticed (fig. 35) that the axial temperature distribution is approximately hyperbolic in form and that the temperature jet-width (fig. 36) increases very nearly linearly with axial distance. A glance at figure 22 or 34 will show that the point at 40 diameters is extremely unreliable.

### Turbulence

The quantity  $u'/U_R$  can scarcely be useful in a flow where instantaneous values of  $u$  are often greater than  $U_R$ . This is certainly the case at the edge of the jet, and therefore it was felt that a dimensionless quantity  $u'/U_m$  proportional to  $u'$ , plotted as a function of radius, would give a more useful picture of the velocity fluctuations in the jet. Further, when the turbulence distributions at various axial positions are to be compared, the quantity  $u'/U_0$  is plotted (fig. 23).

It can be seen from figure 23 that the local minimum at the center of the turbulence distributions does not disappear before an axial distance of about 20 diameters. Thus, although similarity of velocity profiles is effectively reached at 8 or 10 diameters, real kinematic similarity is not reached until about 20 diameters.

It is also interesting to note that the local maximums in the curves for  $x \leq 20$  diameters remain at about the same radius independent of axial position and that this radius is approximately the nozzle mouth radius. Of course, the rather arbitrary curve fairing determines the exact location of the peaks. However, this matter is related to the problem of the evolution from a rectangular velocity profile with very low turbulence to the fully developed turbulent jet, which still awaits an adequate basic experimental investigation.

The axial distribution of  $u'/U_0$  is plotted on figure 35, and although a straight line has been drawn tentatively through three points, the points do not indicate a simple power law.

As mentioned previously, the curves of figure 23 give a clear picture of the spread of the turbulent kinetic energy. Of course, there is a continuous generation of turbulent kinetic energy from the kinetic energy of the mean flow. A quantitative picture of the kinetic energy history of the jet is gotten by integrating the squares of the velocity profiles and the squares of the curves on figure 23. The turbulent kinetic energy in the lateral fluctuations ( $v$ ) is gotten from the  $v'$  distribution measured at  $x = 20$  diameters. It has then been assumed that at all the other stations the  $v$ -energy is in the same ratio to the  $u$ -energy as at 20 diameters. Also, the total  $w$ -energy at a section is taken as equal to the  $v$ -energy for the purpose of this calculation.

The results are plotted on figure 37. The total kinetic energy  $E_T$  and the kinetic energy of the mean flow  $E_M$  crossing a section in unit time are plotted against axial position. The difference between these two curves is the kinetic energy of the turbulent fluctuations  $E'$ . The third curve gives the fraction of the total kinetic energy that consists of turbulent energy, at a section. This curve seems to approach a constant value approximately where the jet achieves complete similarity. At large axial distances, however, it apparently begins to drop off. It is possible that this is merely experimental scatter. The deviation at  $x = 40$  diameters is also clearly visible on figure 38, which is a logarithmic plot of the total, the mean flow, and the turbulent kinetic energies.

### Shear

The turbulent shear is proportional to the  $\overline{uv}$  correlation at a point, which is plotted in dimensionless form at the bottom of figure 25. From this it is seen that the turbulent shear drops off more rapidly along a radial line than does the mean velocity. The ratio of turbulent shear to laminar shear is of more practical significance, and this is plotted on figure 39. In the computation of the laminar shear the velocity profile slopes have been determined graphically so that a sizable probable error has been introduced, particularly near the center of the jet. In fact, it is possible that the maximum located off the axis is merely due to scatter.

From figure 39 it can be seen that in the radial direction the turbulent and laminar shears reach the same order of magnitude before the mean velocity reaches zero. This is one of the indications that the flow is not completely turbulent out to the edge of the jet. The correlation coefficient  $R_{uv}$ , plotted on figure 25, reaches a maximum value of about 0.42. Wattendorf's maximum of 0.33 and Reichardt's maximum of 0.24, both computed by Von Kármán (reference 11) for pipe flow, are values of  $\frac{uv}{u^2}$  instead of  $\frac{uv}{u'v'}$ . The maximum value of  $\frac{uv}{u^2}$  at this cross section in the jet is 0.34.

The extreme scatter near the edge of the jet apparently is due to the fact that in this region one factor in the calculation of  $R_{uv}$  is a small difference between large quantities each of which already has the normal amount of experimental scatter. This excessive scatter may be taken also as an indication that the flow in this region is not continuously turbulent. The dotted part of the curve has no significance and is put in only for completeness.

Mr. Lin has given a method of calculating the total shear at a section from the velocity profile. The method is presented in appendix I, and a comparison between the total shear computed in this way and the experimentally determined shear is given in figure 40. For the latter, only the turbulent shear need be plotted, since the laminar component is negligible in the range for which the points are given. The curves agree very well in shape, although the reason for the discrepancy in magnitude toward the edge of the jet is not evident.

It is worth remarking here that the radial mixing-length distribution, computed from the measured turbulent shear by the assumptions of the momentum transfer theory, shows a maximum deviation of only  $\pm 25$  percent from the average value for the range  $0.2 r_0 < r < 1.8 r_0$ . The curve is plotted in figure 41. As in the case of figure 39, the apparently complex nature of the curve, with two extremes on one side of the axis, may be due to the method of obtaining the results, which includes a graphical determination of the velocity profile slopes.

### Scale of Turbulence

The measurement of the  $\overline{u_1 u_2} / \overline{u^2}$  correlation-coefficient curve, symmetrical about the jet axis at 20 diameters (fig. 26), served a double purpose. First, it gave the scale of turbulence at a "point" in the jet. Second, it showed that there existed no instability of the jet as a whole, such as would cause whipping and therefore an additional negative correlation between points on opposite sides of the jet.

### CONCLUSIONS

1. In a fully developed turbulent jet with axial symmetry, a completely turbulent flow exists only in the core region out to the radius at which the velocity is about one-half the maximum velocity at the cross section. Outside of this core is a wide annular transition region, and from the outside of that to the edge of the jet the flow is in the nature of a laminar collar.
2. In a turbulent heated jet the temperature diffuses more rapidly than the velocity, as also has been recorded in all previously published results.
3. None of the existing turbulence theories gives a satisfactory quantitative relationship between the spread of velocity and the spread of temperature.
4. If theoretical and experimental velocity profiles are matched at the radius where the velocity has one-half its maximum value at the section, the theoretical curve resulting from the assumption of a constant effective shear coefficient gives the best agreement with experiment over the fully turbulent core of the jet, which is the only region where turbulence theories may be expected to apply.
5. Reasonably good similarity of velocity and turbulence profiles in an axially symmetrical jet is not reached until an axial distance of at least 20 diameters where the profile of turbulence  $u' / U_m$  loses its local minimum on the jet axis.

The non-hyperbolic nature of the axial velocity distribution, however, indicates the possibility that even then the similarity is only approximate.

6. In a heated axially symmetrical jet, the dimensionless temperature distribution across a section near the orifice is narrower at the top and wider at the bottom than the corresponding dimensionless velocity distribution. At large axial distances, the temperature profile is everywhere wider than the velocity. The common boundary of these two regions is at an axial distance of about 7 orifice diameters.

This checks the known result that the effective heat-transfer coefficient is greater than the effective-shear coefficient.

California Institute of Technology,  
Pasadena, Calif., June 1943.

#### APPENDIX I

#### CALCULATION OF SHEAR DISTRIBUTION FROM VELOCITY PROFILE

Consider the "boundary-layer form" of the Navier-Stokes equation in cylindrical coordinates:

$$U \frac{\partial U}{\partial x} + v \frac{\partial U}{\partial r} = \frac{1}{\rho r} \frac{\partial}{\partial r} (r \tau) \quad (1)$$

The equation is transformed in the conventional fashion, by assuming similarity, changing to an independent variable  $\eta = \frac{r}{x}$ , and taking a stream function in the form  $\psi = Ax F(\eta)$ , where  $A$  is a constant. The velocity components are then

$$U = \frac{1}{r} \frac{\partial \psi}{\partial r} = \frac{AF'}{x\eta} \quad (2)$$

(2)

$$v = - \frac{1}{r} \frac{\partial \psi}{\partial x} = \frac{A}{x} \left\{ F_1 + \frac{F}{\eta} \frac{F}{\eta} \right\}$$

Next, an expression for the shear is assumed:

$$\tau = B \rho x^{n-1} f(\eta) \quad (3)$$

Substituting equations (2) and (3) into (1) and simplifying the resulting equation gives

$$\frac{A^2}{x^3} \left\{ -\frac{F'^2}{\eta^2} - \frac{F}{\eta} \frac{d}{d\eta} \left( \frac{F'}{\eta} \right) \right\} = \frac{nB}{\eta} x^{n-2} \frac{d}{d\eta} (\eta f) \quad (4)$$

and now  $n = -1$  is chosen so that  $x$  disappears from the equation, and the similarity requirement is satisfied. Combining the two terms on the left side, and multiplying through the equation by  $\eta$ :

$$A^2 \frac{d}{d\eta} \left( \frac{FF'}{\eta} \right) = B \frac{d}{d\eta} (\eta f)$$

which immediately integrates as

$$f = \frac{A^2}{B} \frac{FF'}{\eta^2} \quad (5)$$

where the constant of integration is zero.

This gives the shear in simplest form:

$$\tau = \rho \frac{A^2}{r^2} FF' \quad (6)$$

although for calculation purposes, a more convenient form is

$$\frac{\tau}{\rho} = \frac{A^2}{x^2} \frac{FF'}{\eta^2}$$

## APPENDIX II

REMARKS ON THE CORRECTION OF HOT-WIRE MEASUREMENTS  
FOR THE EFFECT OF TURBULENCE

If  $U$  is defined as the true mean velocity (neglecting  $V$  and  $W$ ),  $u$ ,  $v$ , and  $w$  as the instantaneous components of the fluctuation velocity and  $q$  as the total velocity at any instant, then

$$q = \sqrt{(U + u)^2 + v^2 + w^2} \quad (1)$$

In using the hot wire as a mean-speed measuring device it is desirable to know  $U$ , but the hot wire actually measures  $\bar{q}$ , and when the turbulence level is sufficiently high some correction must be applied.

The relationship between  $\bar{q}$  and  $U$  may be obtained by writing

$$\bar{q} = U \sqrt{1 + 2 \frac{\bar{u}}{U} + \left(\frac{\bar{u}}{U}\right)^2 + \left(\frac{\bar{v}}{U}\right)^2 + \left(\frac{\bar{w}}{U}\right)^2} \quad (2)$$

or, by letting

$$v^2 + w^2 = (\alpha - 1) u^2$$

$$\bar{q} = U \sqrt{1 + 2 \frac{\bar{u}}{U} + \alpha \left(\frac{\bar{u}}{U}\right)^2} \quad (3)$$

and expanding the radical out to terms in  $\left(\frac{\bar{u}}{U}\right)^4$

$$\bar{q} = U \left\{ 1 + \frac{1}{2}(\alpha - 1) \left(\frac{\bar{u}}{U}\right)^2 - \frac{1}{2}(\alpha - 1) \left(\frac{\bar{u}}{U}\right)^3 - \frac{1}{8}(\alpha^2 - 6\alpha + 5) \left(\frac{\bar{u}}{U}\right)^4 \right\} \quad (4)$$

since  $\bar{\dot{u}} = 0$ .

This expansion converges only for

$$\left[ 2 \frac{u}{U} + \alpha \left( \frac{u}{U} \right)^2 \right]^2 \ll 1$$

If equation (3) is rewritten in the form

$$\bar{q} = U \left[ \left( 1 + \frac{u}{U} \right) \sqrt{1 + (\alpha - 1) \left( \frac{u}{U} \right)^2} \right] \quad (5)$$

an expansion convergent for

$$\left[ (\alpha - 1) \left( \frac{u}{U} \right)^2 \right]^2 \ll 1$$

can be obtained.

It must be remembered that  $u/U$  is a fluctuating quantity with a distribution probably similar to the Gaussian and symmetrical about zero. This means that the convergence requirements must be met by the main body of the distribution, if not by the edges.

The principal difficulty with such a theoretical correction is that the values of  $\left( \frac{u}{U} \right)^n$  are unknown for the integer  $[n] > 2$ . Therefore, the expansion cannot be computed to any desired accuracy. If all powers of  $u/U$  higher than the second are omitted, the expansions of equations (3) and (5) give the same result. If, then, it is assumed that  $\alpha = 2$

$$U = \frac{\bar{q}}{1 + 2 \left( \frac{u}{U} \right)^2} \quad (6)$$

which is plotted in figure 42. This must be considered as a qualitative rather than a quantitative correction.

A similar attack on the problem of correcting hot-wire turbulence-level readings for the effect of the turbulence upon the instrument meets with even greater difficulties. Thus, it would appear that an experimental approach to both problems would be more fruitful.

Up to the present time, no measurements have been made at the GALCIT to determine the effect of turbulence upon mean-speed readings, but some preliminary measurements have been carried out on the effect of turbulence upon hot-wire readings of the turbulence.

The procedure was to vibrate a hot wire sinusoidally in the flow direction of a relatively low-turbulence air stream. The vibrating device was the GALCIT vibrator, constructed by F. Knoblock and C. Thiele in 1937 for the purpose of determining hot-wire time-constants to permit proper compensation for thermal lag. The hot-wire circuit was properly compensated and the true turbulence level determined by measurement of the amplitude and frequency of the oscillation and the speed of the air stream.

A comparison between the true and the measured turbulence levels is given in figure 43 for the same hot wire and three different speeds. It is surprising to notice that the curve is concave upward for a range before the main drop-off begins. The appreciable deviation of the points at the highest speed indicates that the curve may be dependent upon the sensitivity or the temperature of the hot wire; and, of course, the applied compensation for thermal lag was correct only for relatively low turbulence levels.

It is hoped that tests may be made in the near future to determine the effects of high turbulence upon the readings of both mean velocity and turbulence level with the hot-wire anemometer.

## REFERENCES

1. Ruden, P.: Turbulente Ausbreitungsvorgänge im Freistrahle. Die Naturwissenschaften, vol. 21, nos. 21/23, May 1933, pp. 375-378.
2. Kuethe, Arnold M.: Investigations of the Turbulent Mixing Regions Formed by Jets. Jour. Appl. Mechanics (A.S.M.E.), Sept. 1935, pp. 87-95.
3. Prandtl, L.: The Mechanics of Viscous Fluids. Vol. III, div. G, of Aerodynamic Theory, W. F. Durand, ed., Julius Springer (Berlin), 1935.
4. Taylor, G. I.: The Transport of Vorticity and Heat through a Fluid in Turbulent Motion. Proc. Roy. Soc. London, ser. A, vol. 135, 1932, pp. 685-702.
5. Chou, P. Y.: On an Extension of Reynolds' Method of Finding Apparent Stress and the Nature of Turbulence. Chinese Jour. of Physics, vol. 4, Jan. 1940.
6. von Kármán, Th.: The Fundamentals of the Statistical Theory of Turbulence. Jour. Aeron. Sci., vol. 4, no. 4, Feb. 1937, pp. 131-138.
7. Tollmien, Walter: Berechnung turbulenter Ausbreitungsvorgänge. Z.f.a.M.M., vol. 6, Dec. 1926, pp. 468-478.
8. Tomotika, S.: Application of the Modified Vorticity Transport Theory to the Turbulent Spreading of a Jet of Air. Proc. Roy. Soc. London, vol. 165, March 18, 1938, pp. 65-72.
9. Howarth, L.: Concerning the Velocity and Temperature Distributions in Plane and Axially Symmetrical Jets. Proc. Cambridge Phil. Soc., vol. 34, 1938.
10. Liepmann, Hans W.: Investigations on Laminar Boundary-Layer Stability and Transition on Curved Boundaries. NACA ACR No. 3H30, Aug. 1943. (Fig. 20)
11. von Kármán, Th.: Some Aspects of the Turbulence Problem. Proc. of the Fourth Int. Congr. for Appl. Mechanics, The Univ. Press (Cambridge) 1935.

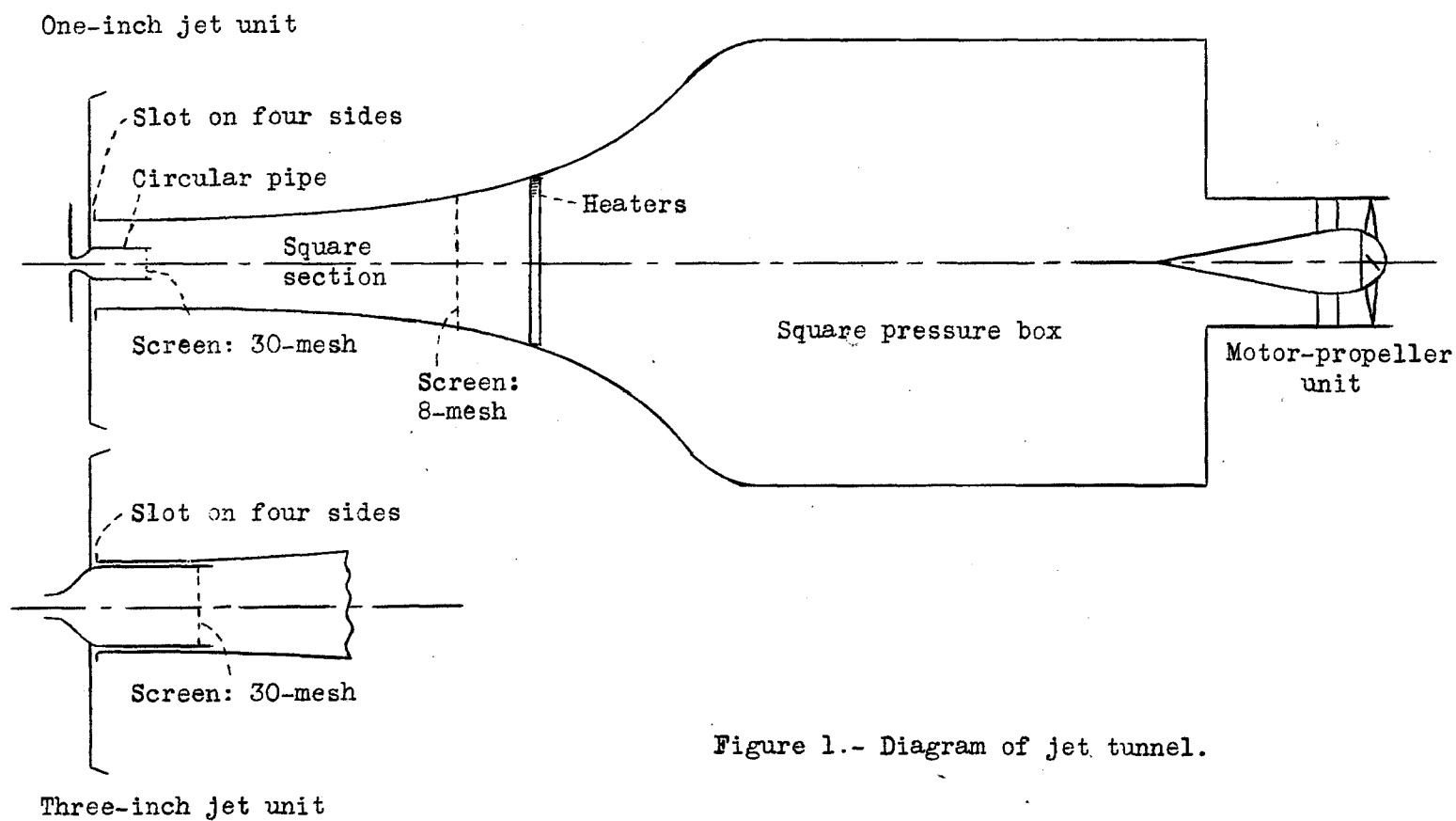


Figure 1.- Diagram of jet tunnel.

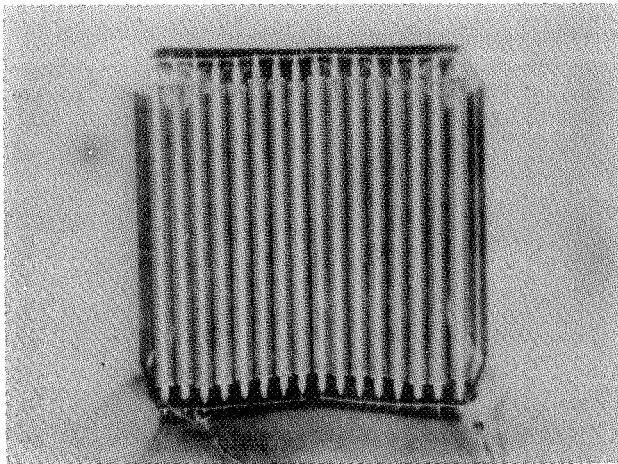


Figure 2.-  
The  
heating  
unit  
mounted  
in the  
main  
tunnel  
contraction.

Figure 3.-  
View  
looking  
upstream  
at motor-  
propeller  
unit from  
inside  
the  
pressure  
box.

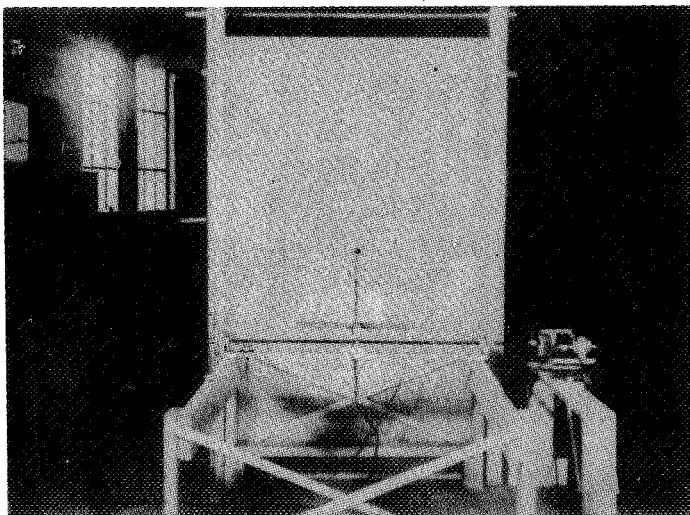
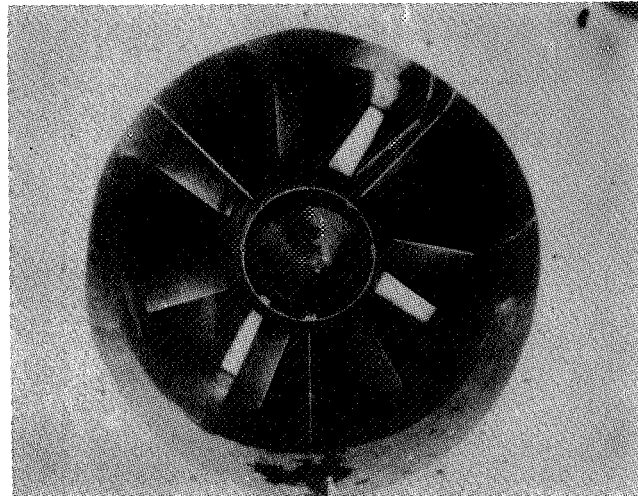


Figure 4.-  
Jet  
orifice  
and  
traversing  
unit from  
downstream  
end of jet.

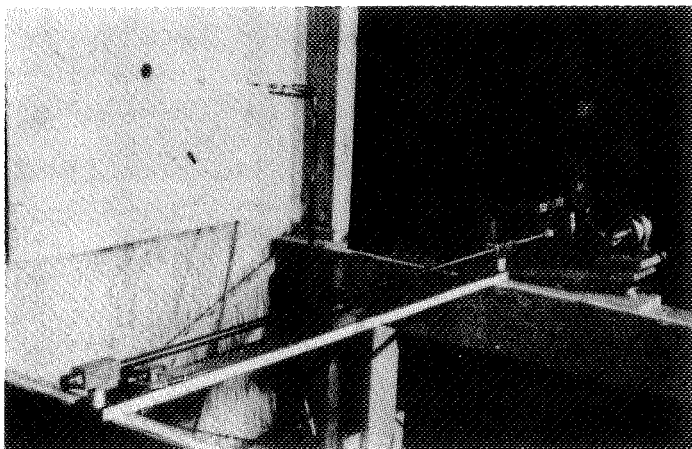


Figure 5.-  
Close-up  
of track,  
drive  
mechanism  
and  
hot-wire  
carriage.

Figure 6.-  
The 4-wire  
2-amplifier  
unit. Aux-  
iliary  
amplifier  
is in a  
separate  
case, not  
in the  
picture.

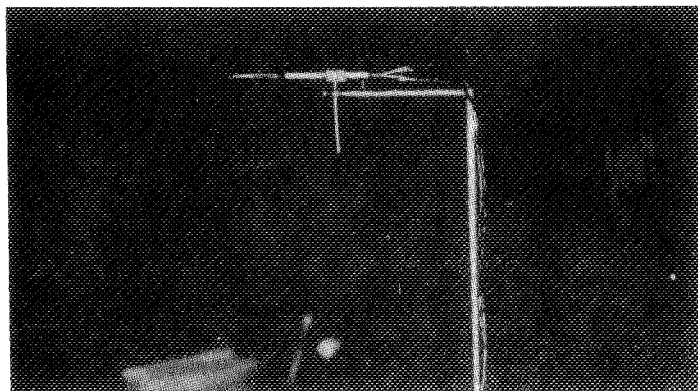
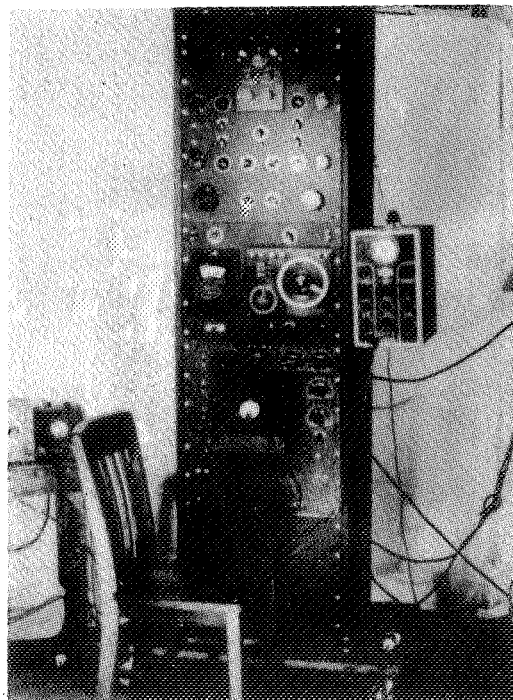


Figure 7.-  
A 2-wire  
uv-meter  
or v-meter  
mounted  
on the  
carriage.  
The carriage  
takes  
ordinary  
u-meters  
with no  
external leads.

THREE-INCH HEATED JET

Axial Distributions  
Along Center Line

Velocity (uncorrected) ———  
" (corrected) - - - - -  
Temperature ———

$U_m$  = mean velocity on axis  
 $U_0$  = " " at mouth  
 $T_m$  = mean temperature on axis  
 $T_0$  = " " at mouth  
 $u$  = axial fluctuation velocity  
 $u' = \sqrt{\overline{u^2}}$

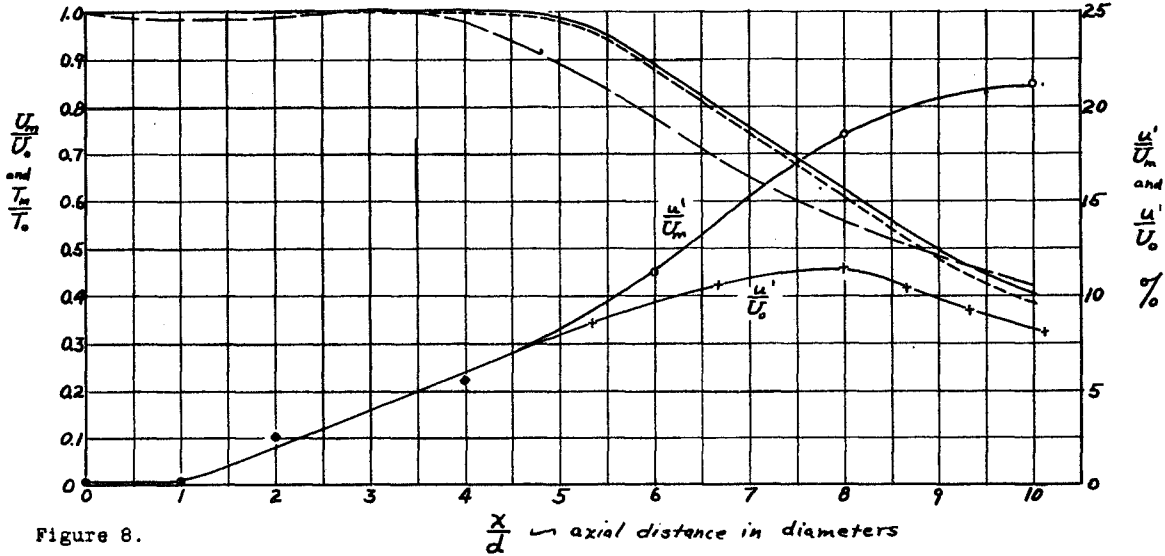


Figure 8.

(1 block = 10 divisions on 1/40" Engr. scale. Hold on slight angle.)

THREE-INCH HEATED JET  
Lateral Traverse at  $X=0$  Diameters

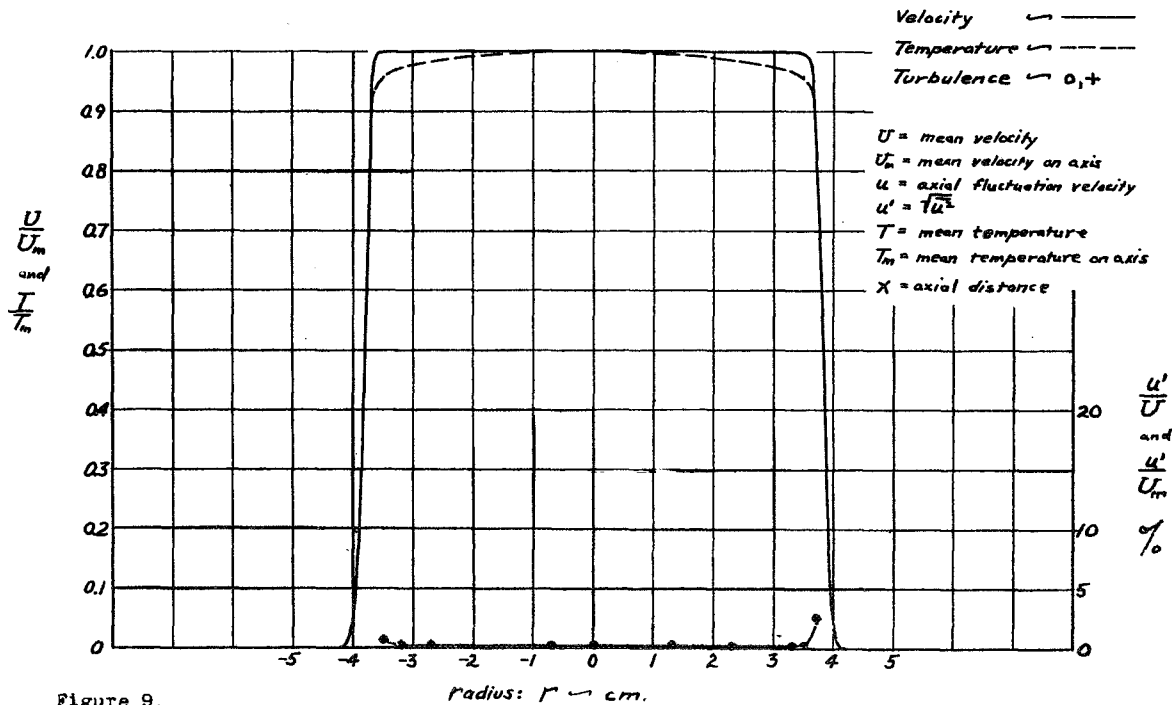


Figure 9.

(1 block = 10 divisions on 1/32" Arch. scale)

THREE-INCH HEATED JET  
Lateral Traverse at X = 1 Diameter

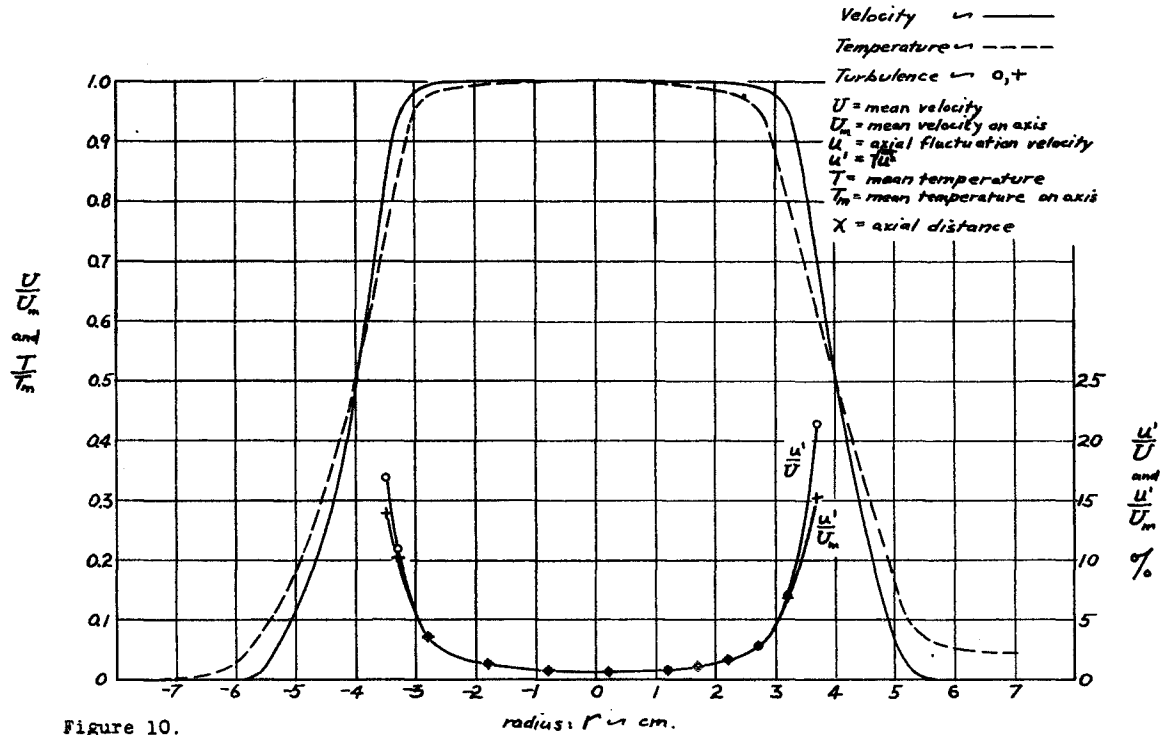


Figure 10.

(1 block = 10/32")

THREE-INCH HEATED JET  
Lateral Traverse at X = 2 Diameters

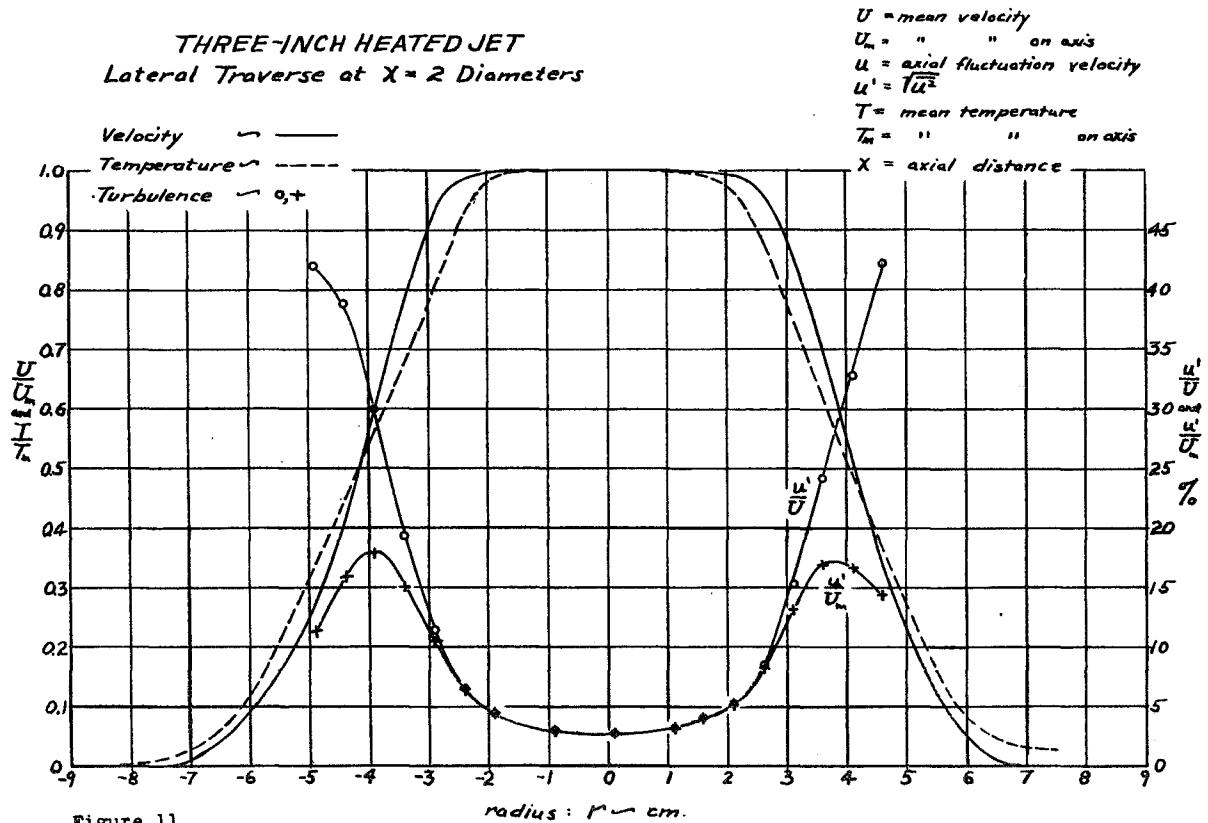


Figure 11.

**THREE-INCH HEATED JET**  
Lateral Traverse at  $X=4$  Diameters

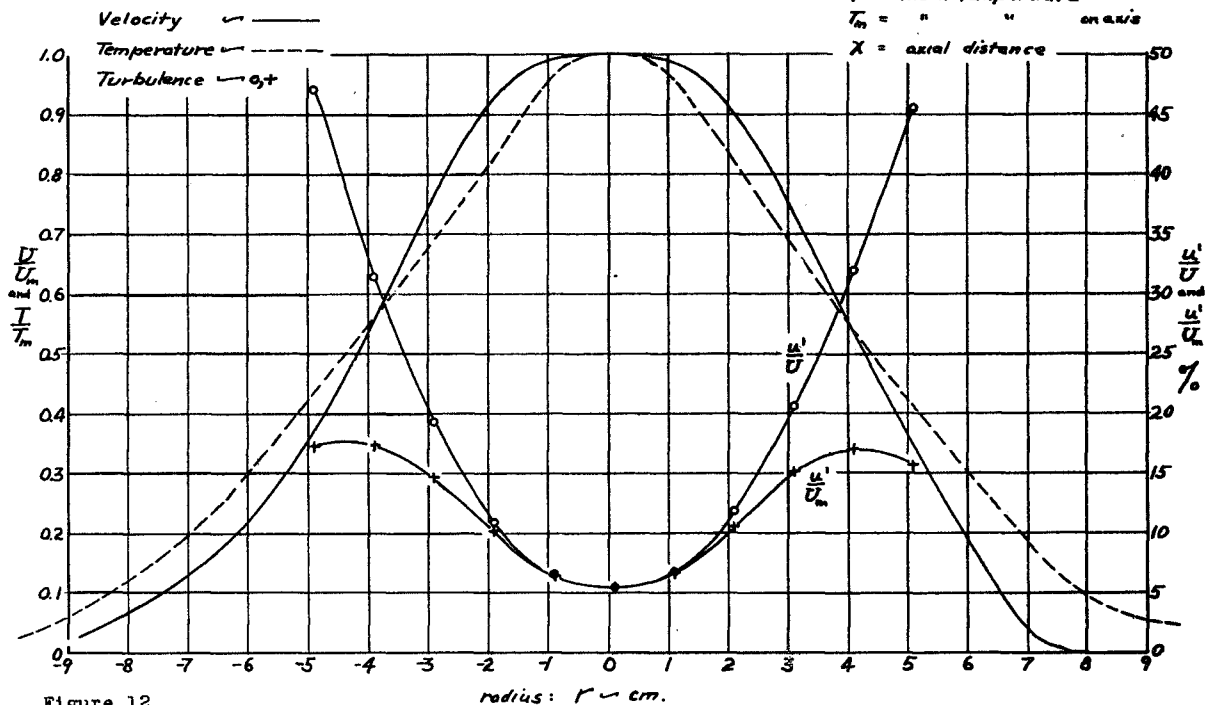


Figure 12.

(1 block = 10/32")

**THREE-INCH HEATED JET**  
Lateral Traverse at  $X=6$  Diameters

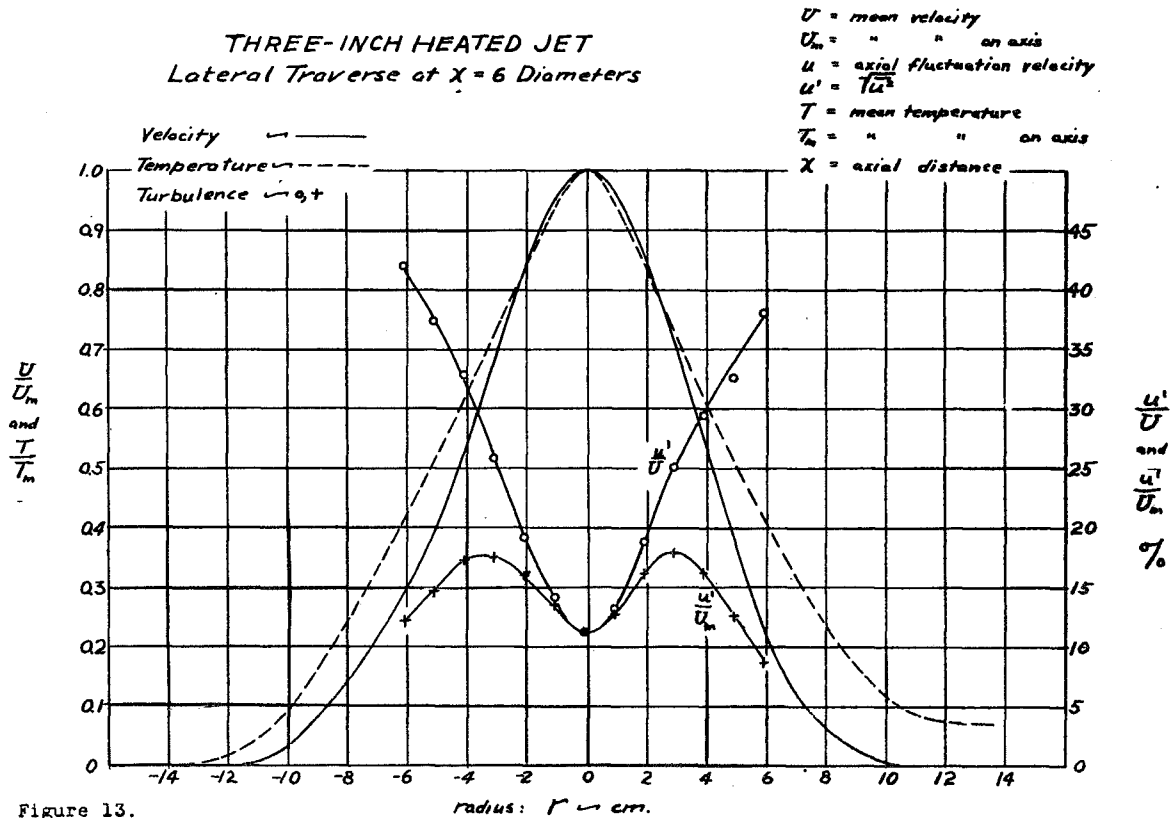


Figure 13.

**THREE-INCH HEATED JET**  
Lateral Traverse at  $X = 8$  Diameters

$U$  = mean velocity  
 $U_m$  = " " on axis  
 $u$  = axial fluctuation velocity  
 $u' = \sqrt{u^2}$   
 $T$  = mean temperature  
 $T_m$  = " " on axis  
 $X$  = axial distance

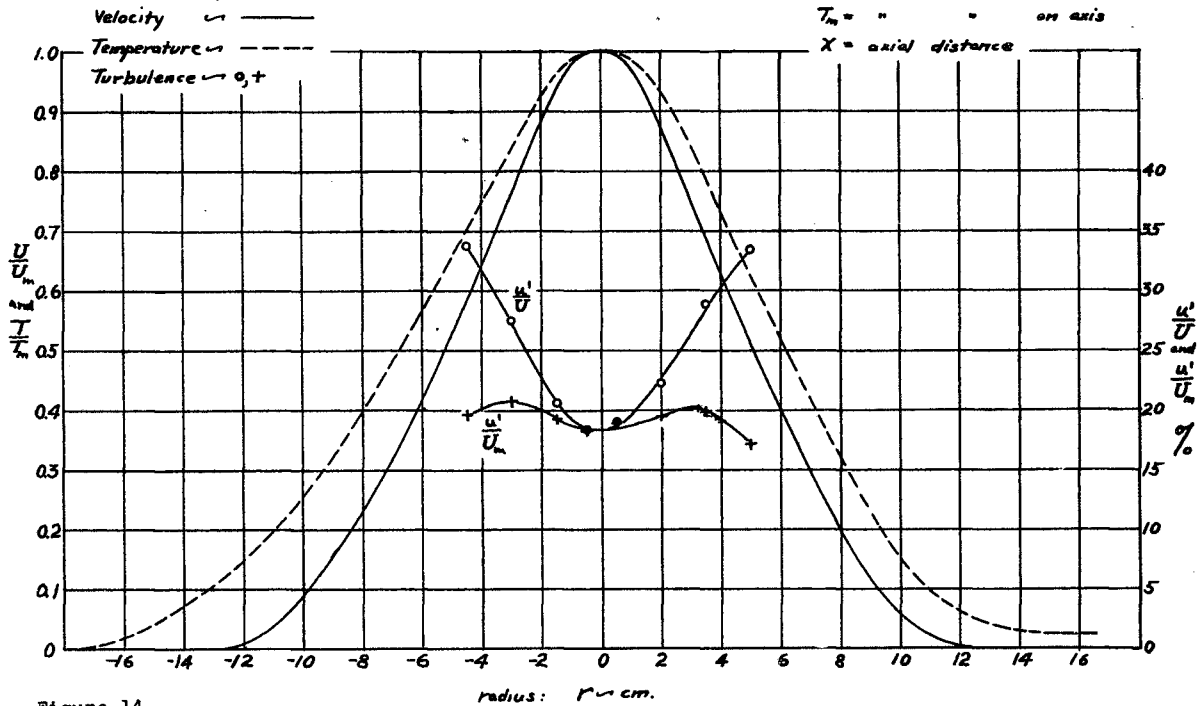


Figure 14.

radius:  $r$  cm.

(1 block =  $10/32''$ )

**THREE-INCH HEATED JET**  
Lateral Traverse at  $X = 10$  Diameters

$U$  = mean velocity  
 $U_m$  = " " on axis  
 $u$  = axial fluctuation velocity  
 $u' = \sqrt{u^2}$   
 $T$  = mean temperature  
 $T_m$  = " " on axis  
 $X$  = axial distance

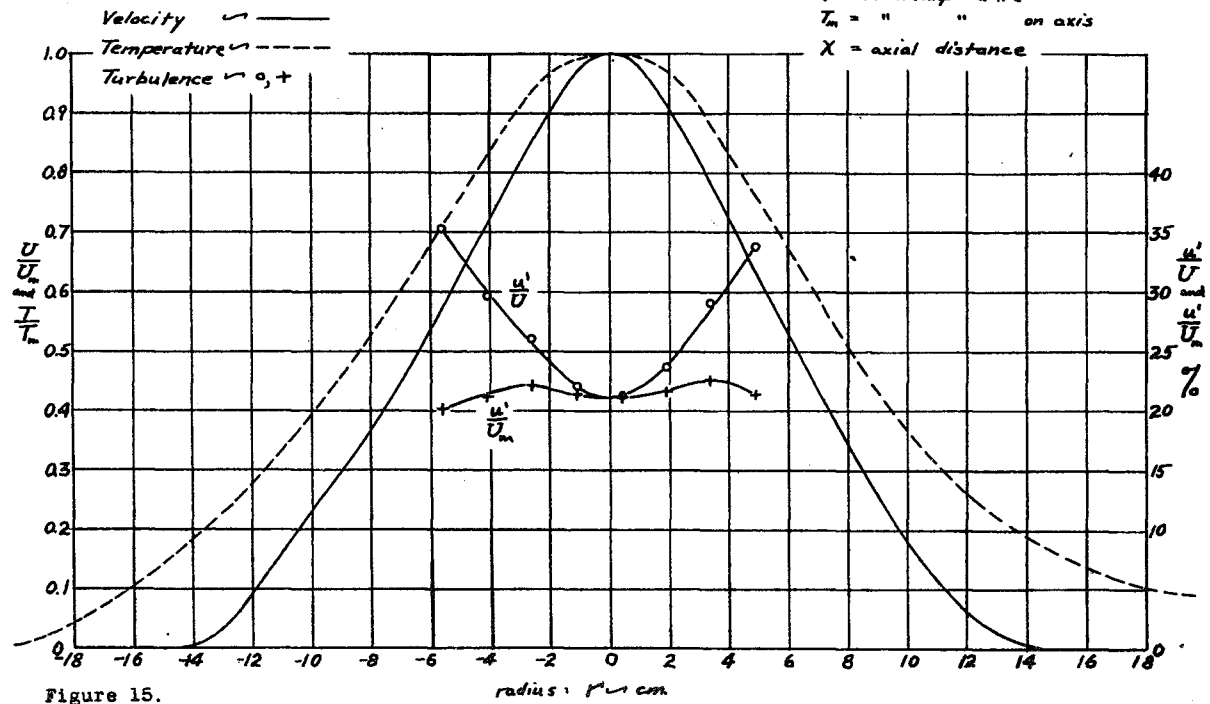


Figure 15.

radius:  $r$  cm.

**THREE-INCH HEATED JET**  
Lateral Traverse at X = 12 Diameters

U = mean velocity Figs. 16,17  
 U<sub>m</sub> = " " on axis  
 u = axial fluctuation velocity  
 u' =  $\sqrt{u^2}$   
 T = mean temperature  
 T<sub>m</sub> = " " on axis  
 X = axial distance

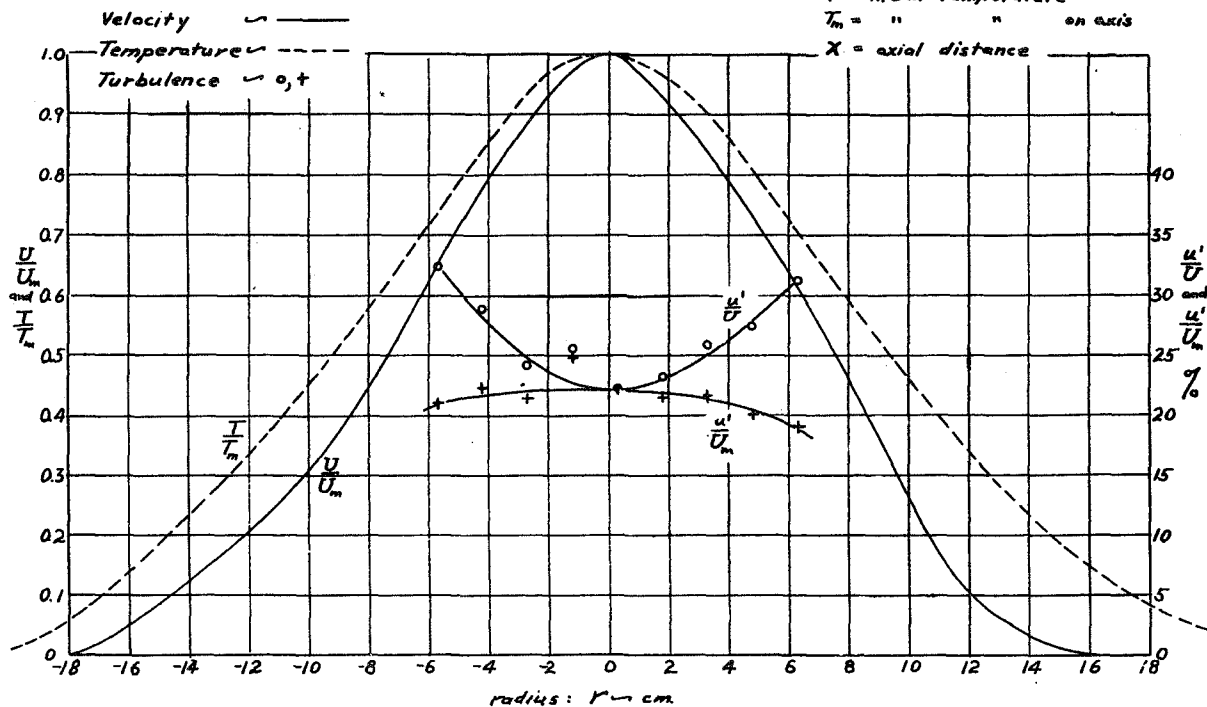


Figure 16.

(1 block = 10/32")

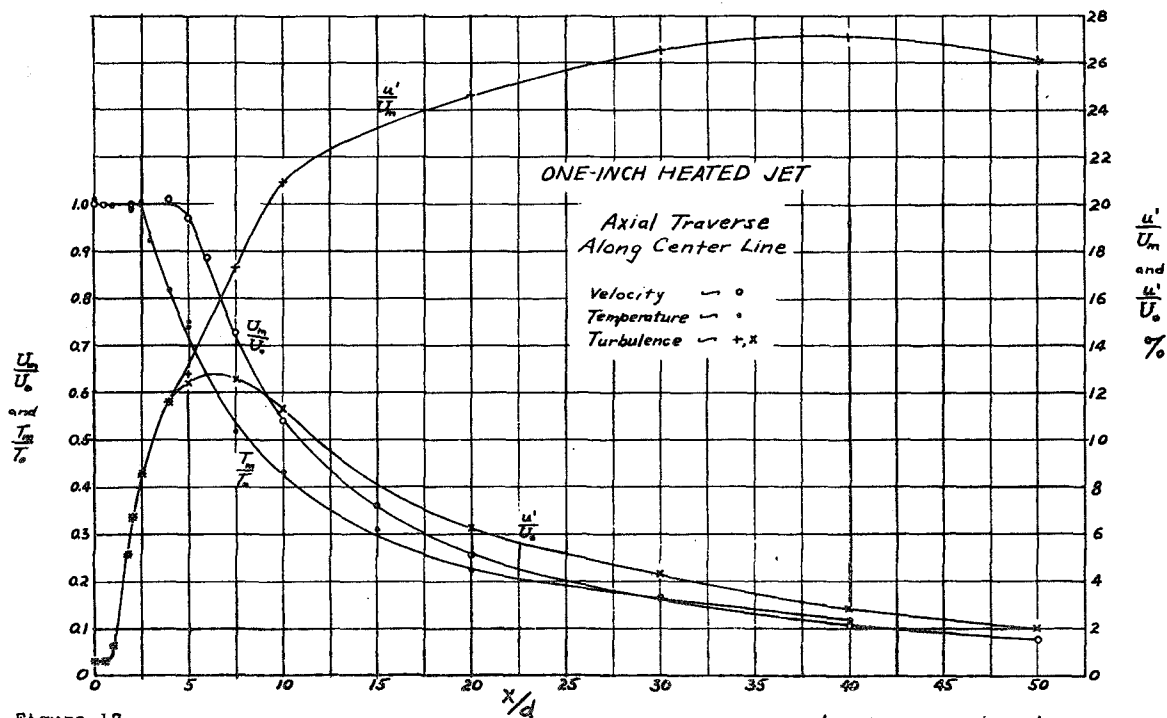
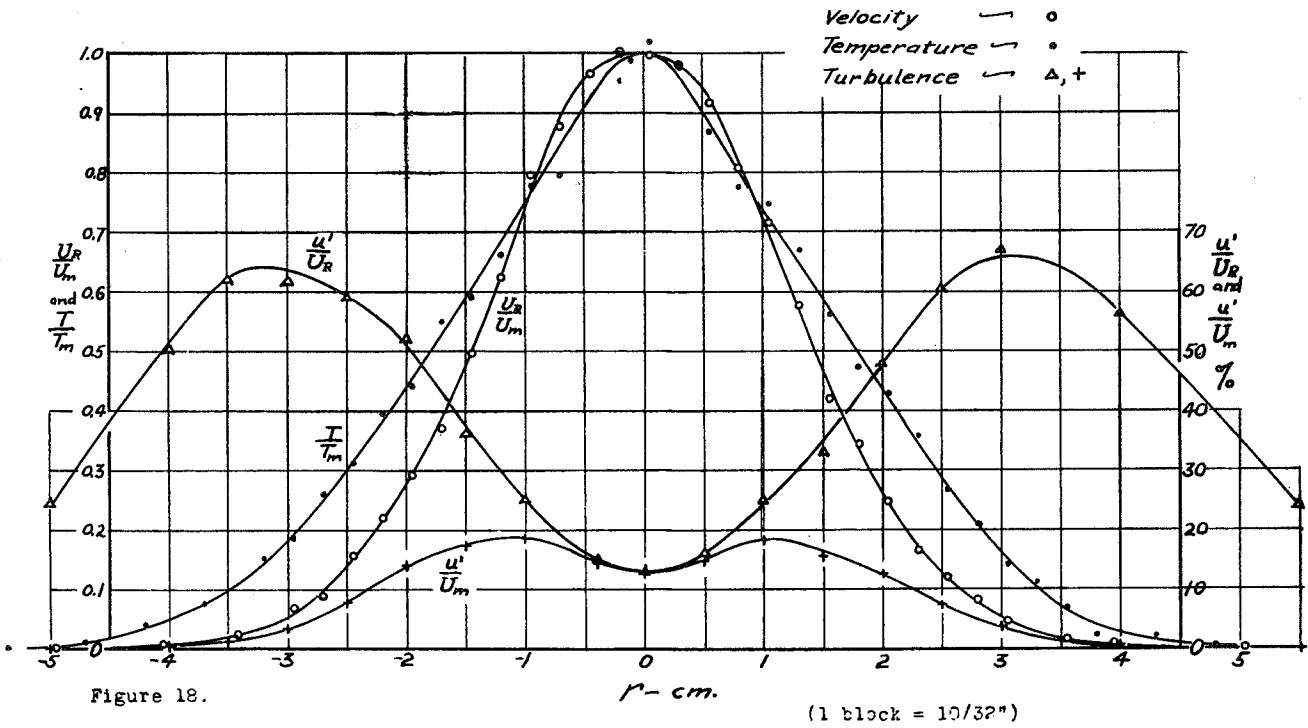


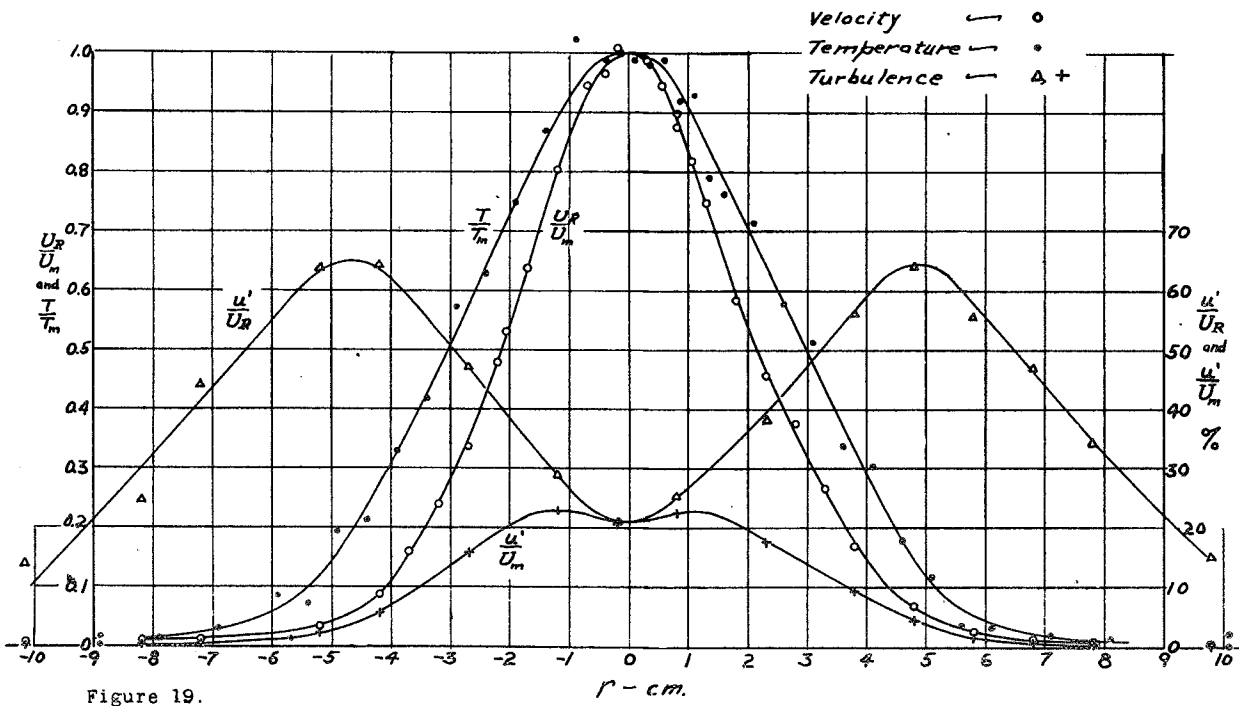
Figure 17.

(1 block = 10/40")

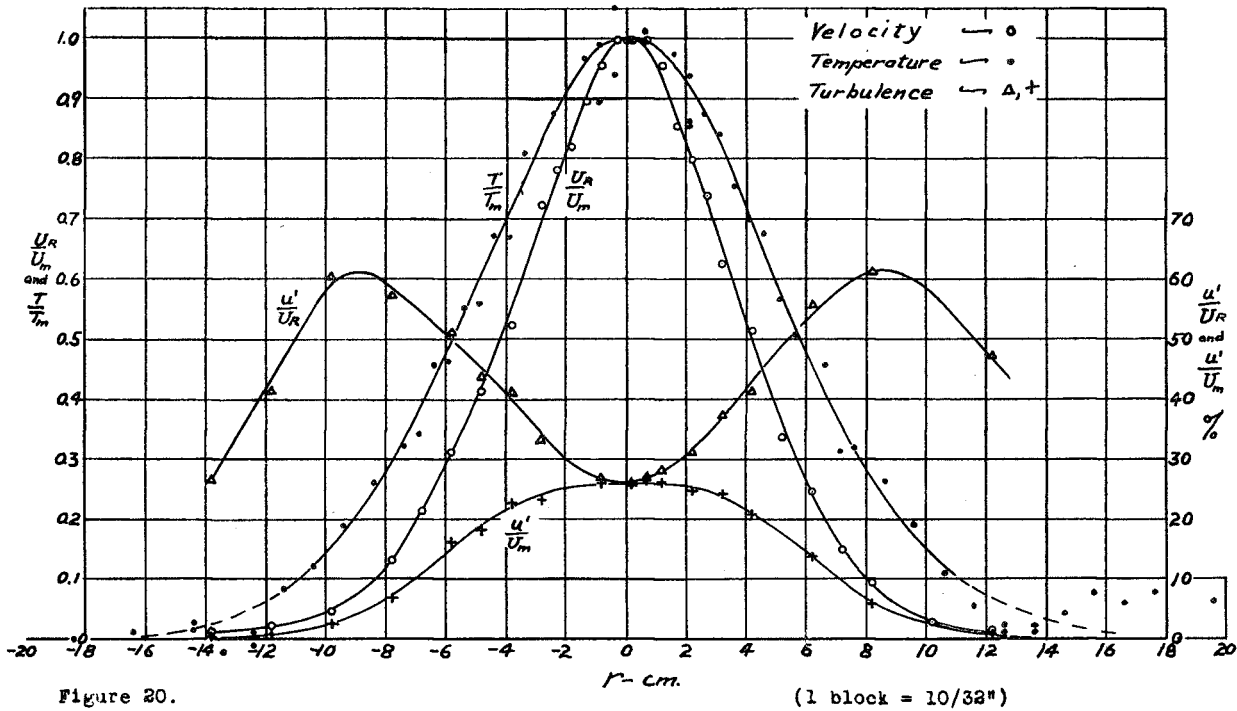
ONE-INCH HEATED JET  
Lateral Traverse at X = 5 Diameters



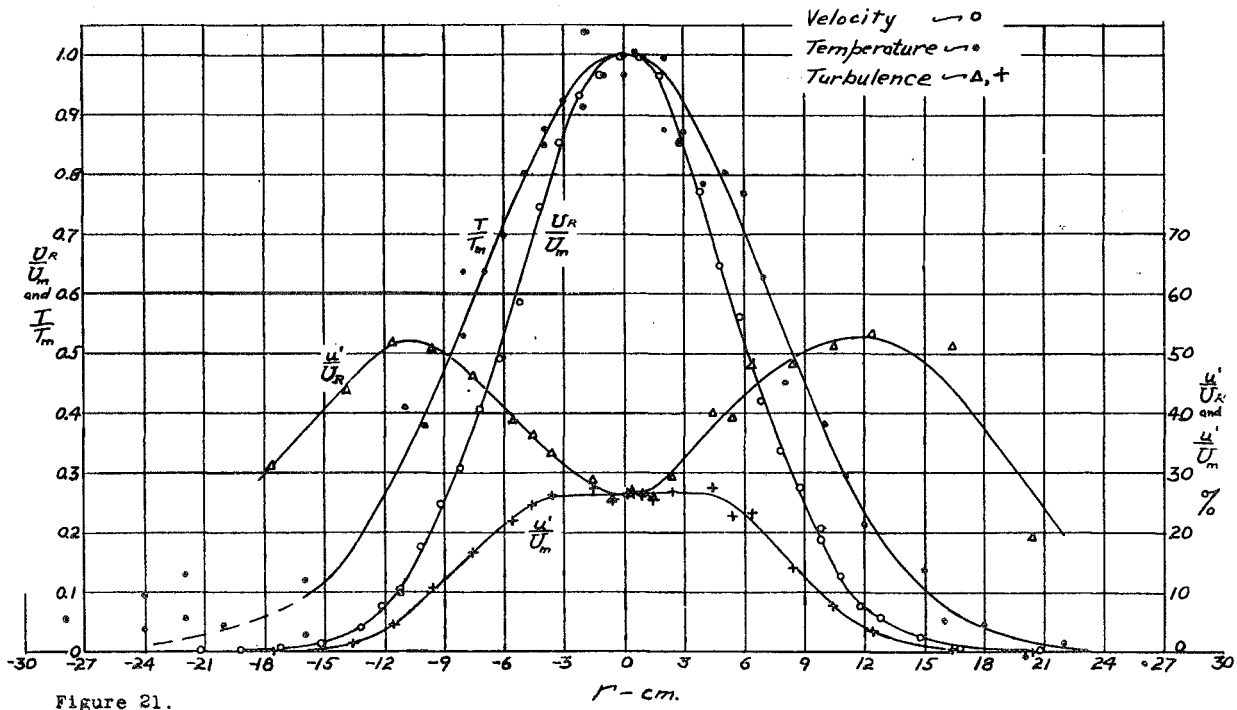
ONE-INCH HEATED JET  
Lateral Traverse at X = 10 Diameters



ONE-INCH HEATED JET  
Lateral Traverse at X = 20 Diameters



ONE-INCH HEATED JET  
Lateral Traverse at X = 30 Diameters



ONE-INCH HEATED JET  
Lateral Traverse at X = 4.0 Diameters

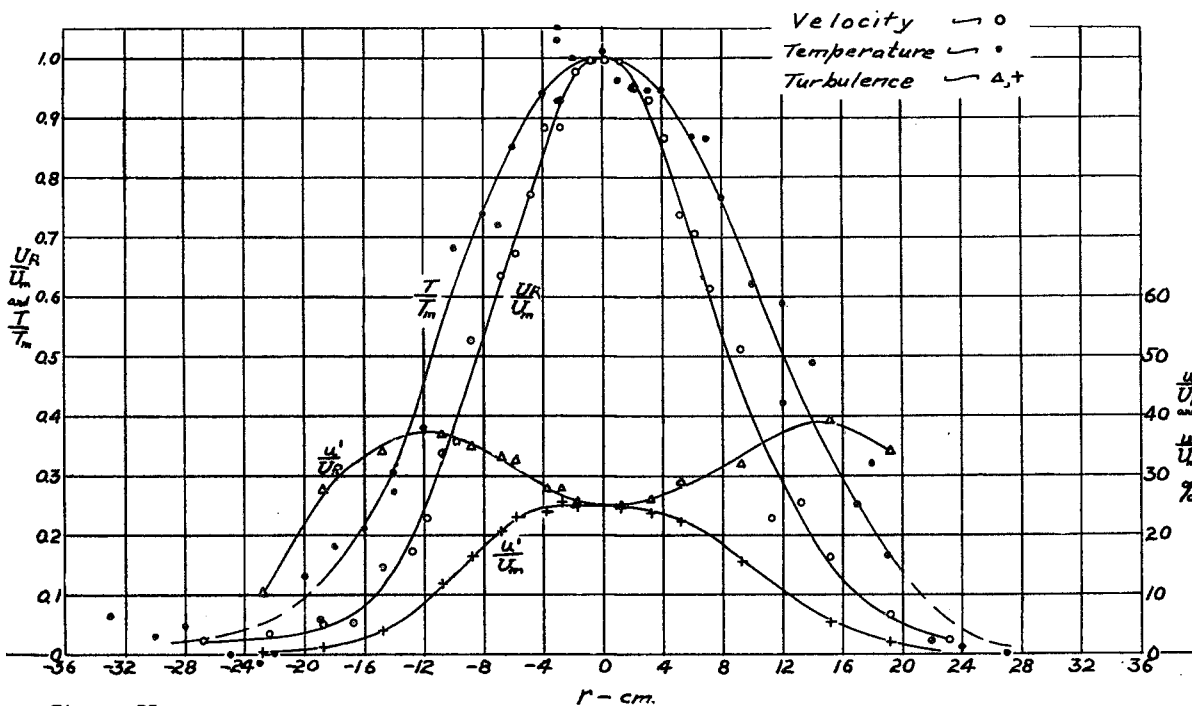


Figure 22.

(1 block = 10/32")

ONE-INCH HEATED JET  
Distributions of Turbulent Velocities

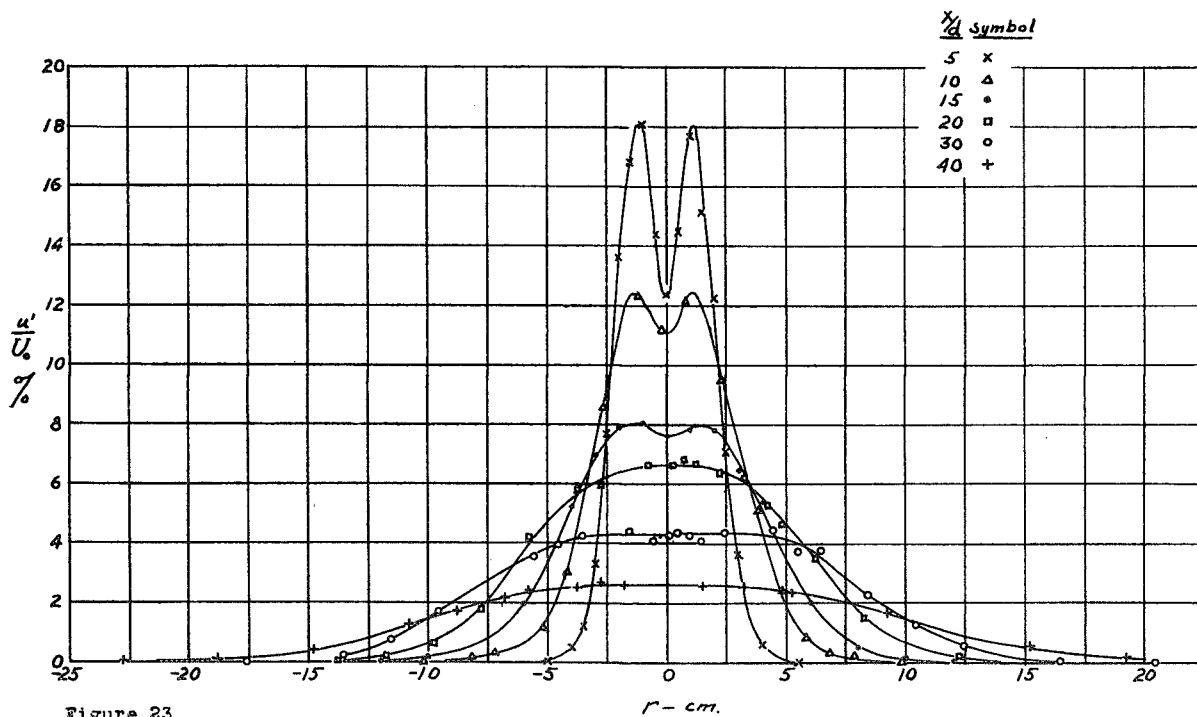


Figure 23.

ONE-INCH HEATED JET  
Comparison of Axial and Radial Turbulence  
 $X = 20$  dia.

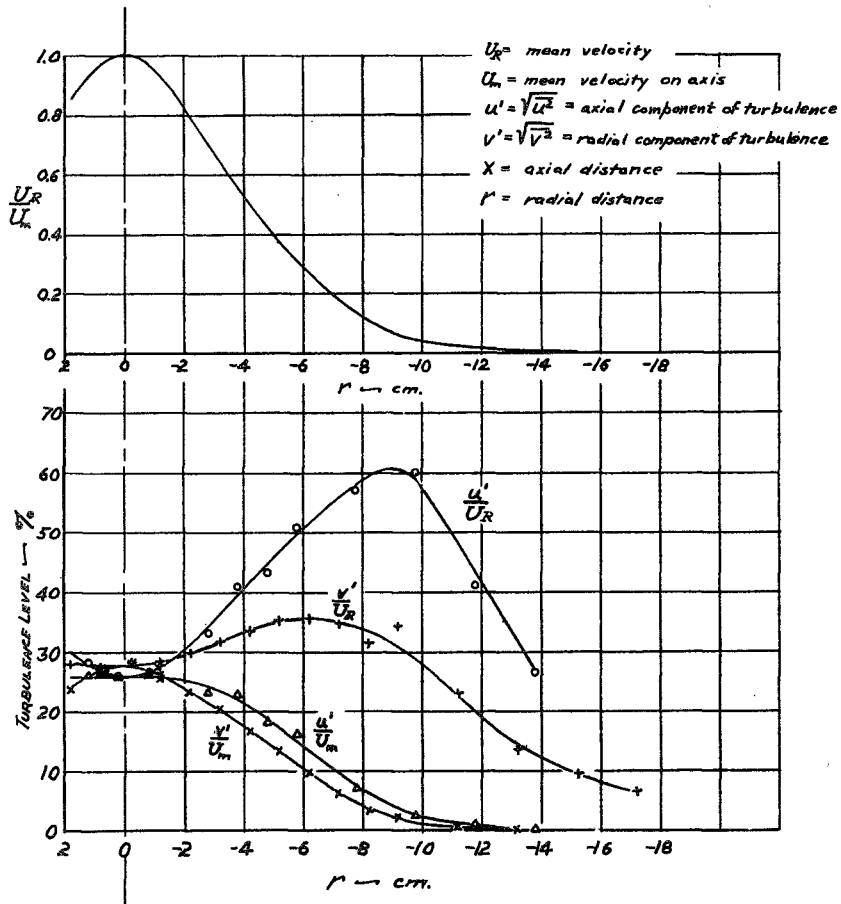


Figure 24.

(1 block =  $10/32''$ )

ONE-INCH HEATED JET  
Double Correlation ( $\overline{uv}$ )  
 $X = 20$  dia.

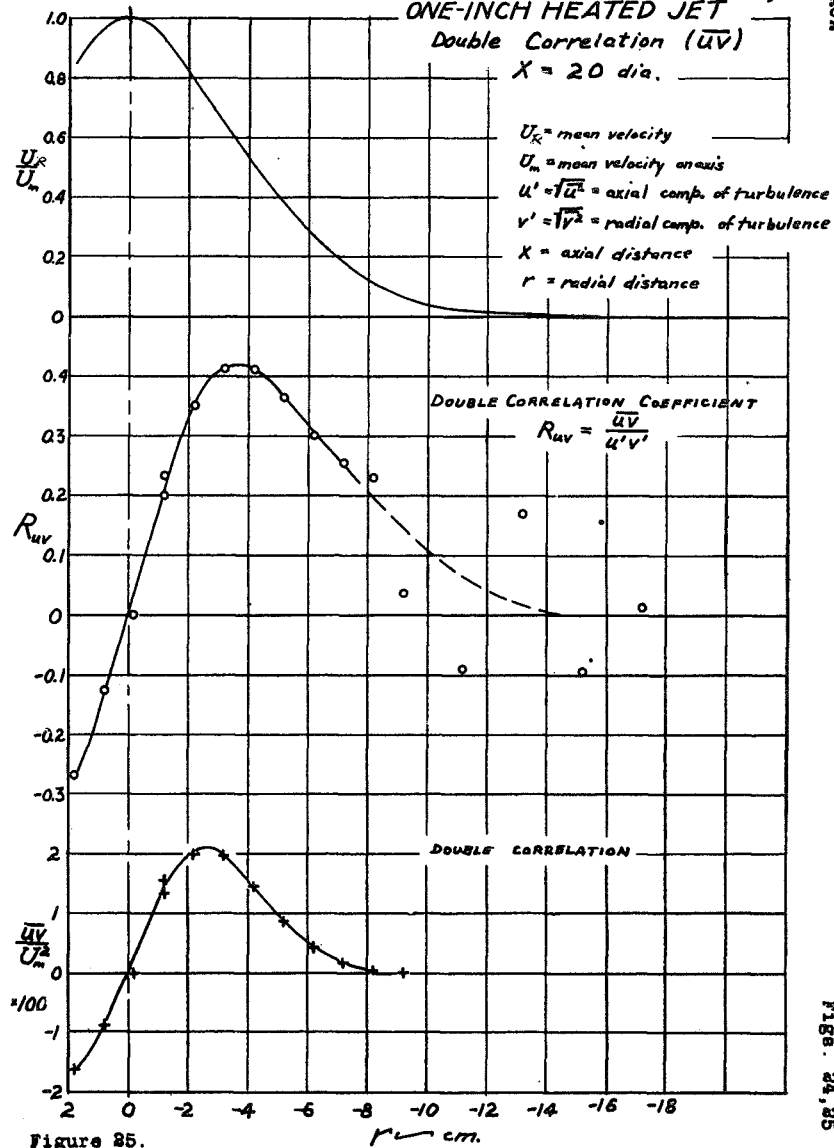


Figure 25.

ONE-INCH HEATED JET

Double Correlation Symmetrical about Axis (i.e.:  $r_1 = -r_2$ )

$X = 20 \text{ dia.}$

$$R(r) = \frac{u_1 u_2}{u^2} = \text{Correlation Coefficient}$$

$r_{12}$  = radial distance of points 1 and 2

$u_{1,2}$  = axial component of turbulent fluctuation of points 1 and 2

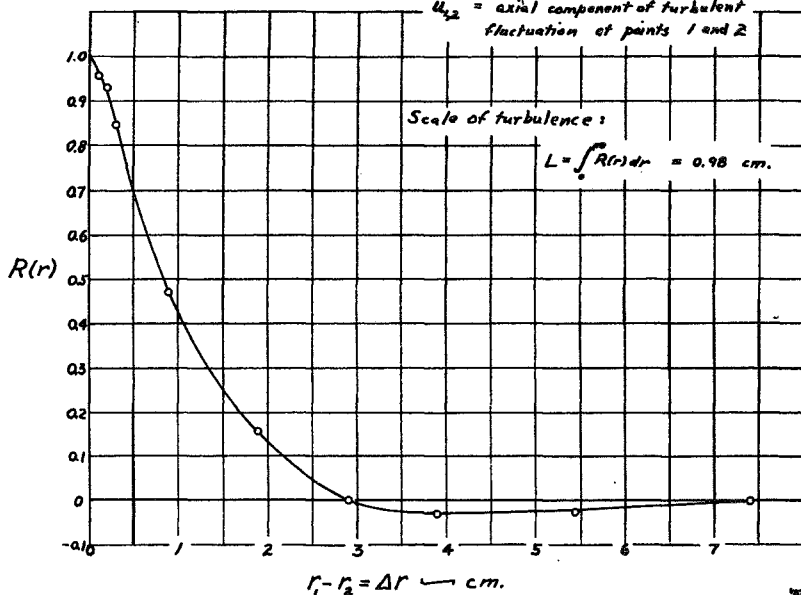
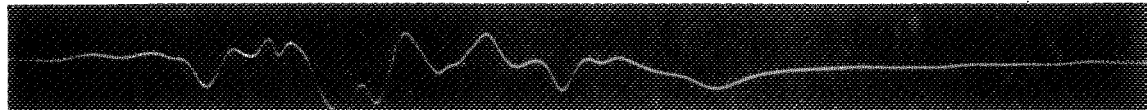
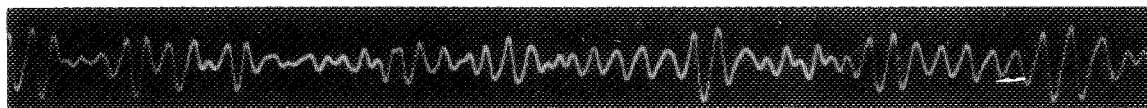


Figure 26.

(1 block =  $10/40^{th}$ )

(a)  $r = 0$  (on axis)(b)  $r = 4.5 \text{ cm} = 1.07 r_0$ (c)  $r = 7.5 \text{ cm} = 1.79 r_0$ (d)  $r = 9.5 \text{ cm} = 2.26 r_0$ (e)  $r = 14.5 \text{ cm} = 3.45 r_0$ Figure 27.- One-inch heated jet,  $x = 20$  diameters.(a)  $r = 0$  (on axis)(b)  $r = 1.27 \text{ cm} = d/2$ 

(c) Timing wave: 200 cps (for figs. 27 and 28)

Figure 28.- One-inch heated jet,  $x = 2$  diameters.

**ONE-INCH HEATED JET**  
*Lateral Velocity Distribution Compared with Theory*  
*X = 5 dia.*

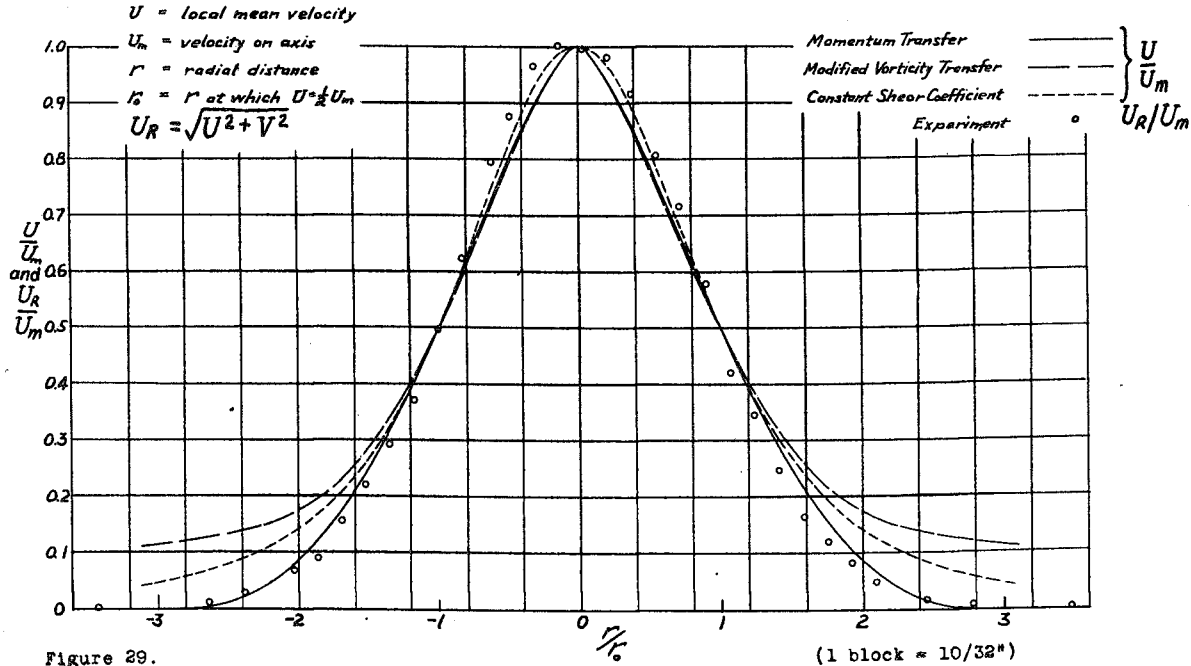


Figure 29.

ONE-INCH HEATED JET  
Lateral Velocity Distribution Compared with Theory  
X = 10, 20 and 30 dia.

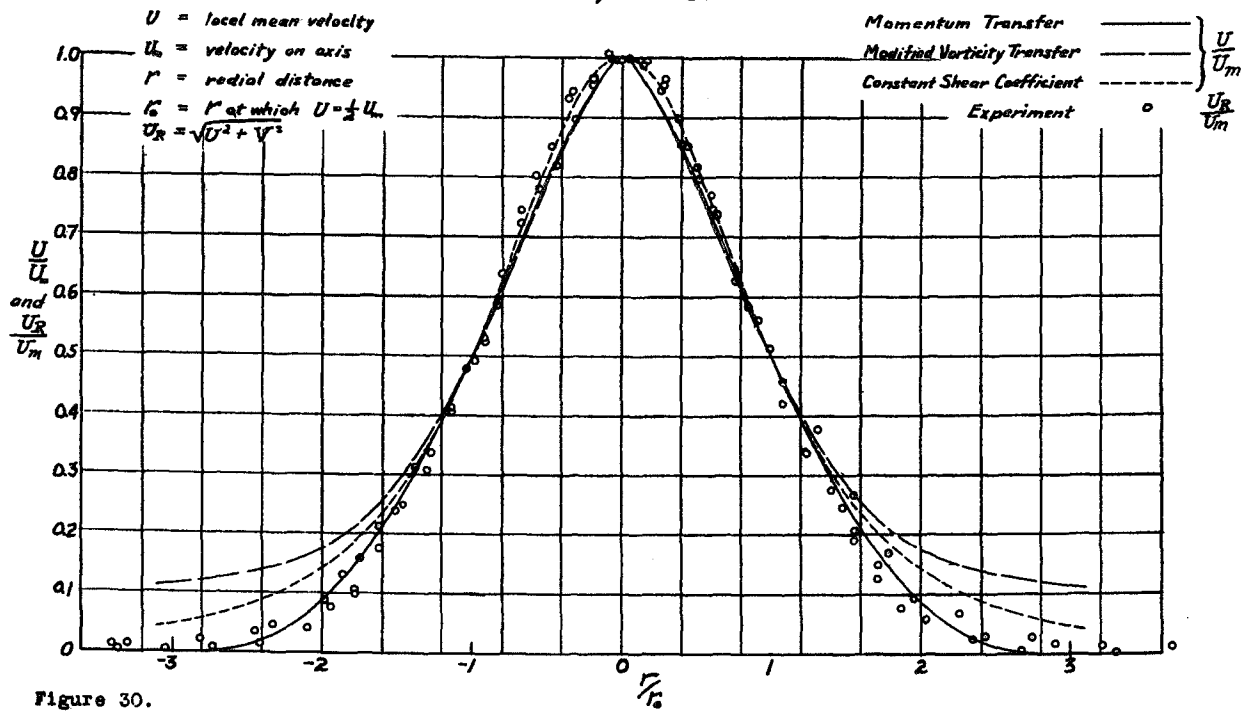


Figure 30.

(1 block = 10/32")

ONE-INCH HEATED JET  
Lateral Velocity Distribution Compared with Theory  
X = 40 dia.

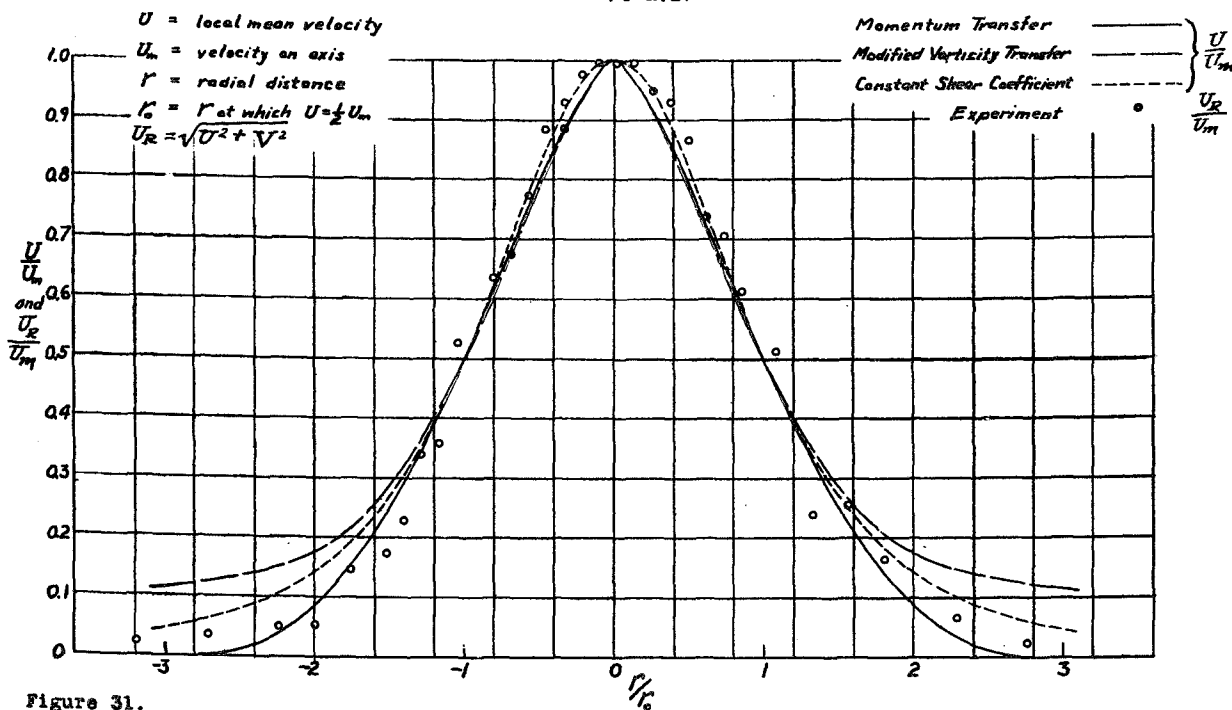


Figure 31.

ONE-INCH HEATED JET  
Lateral Temperature Distribution Compared with Theory  
 $X = 5$  dia.

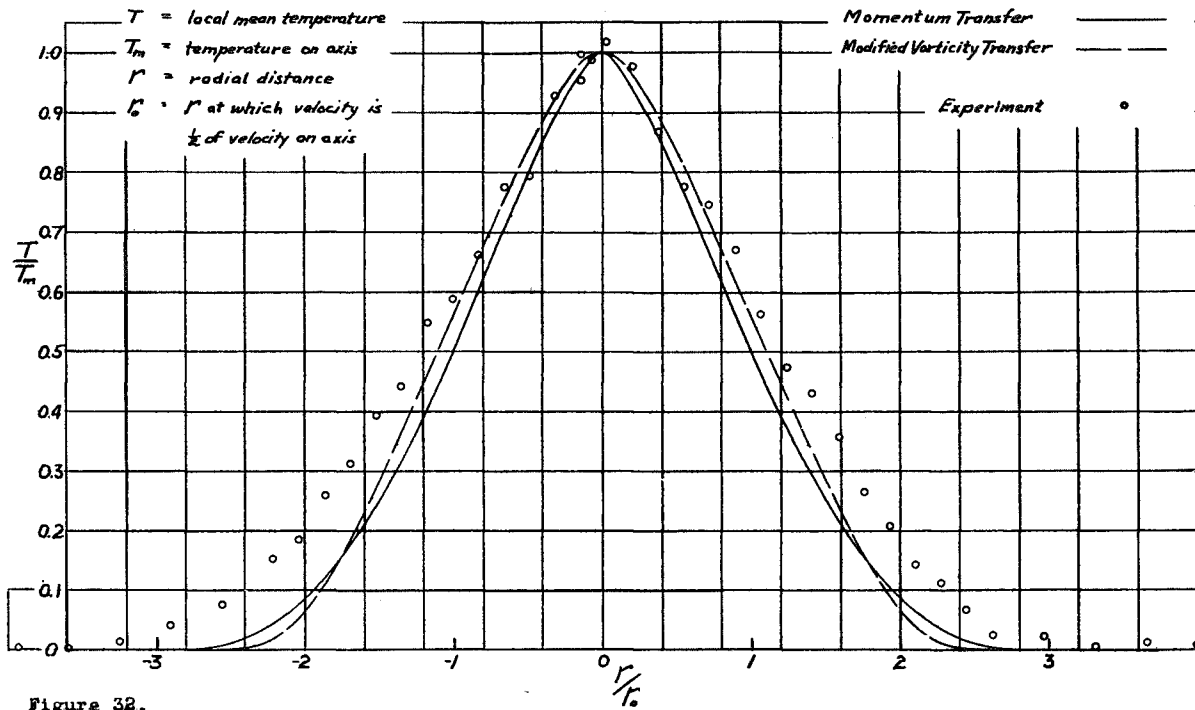


Figure 32.

(1 block = 10/32")

ONE-INCH HEATED JET  
Lateral Temperature Distribution Compared with Theory  
 $X = 10, 20$  and  $30$  dia.

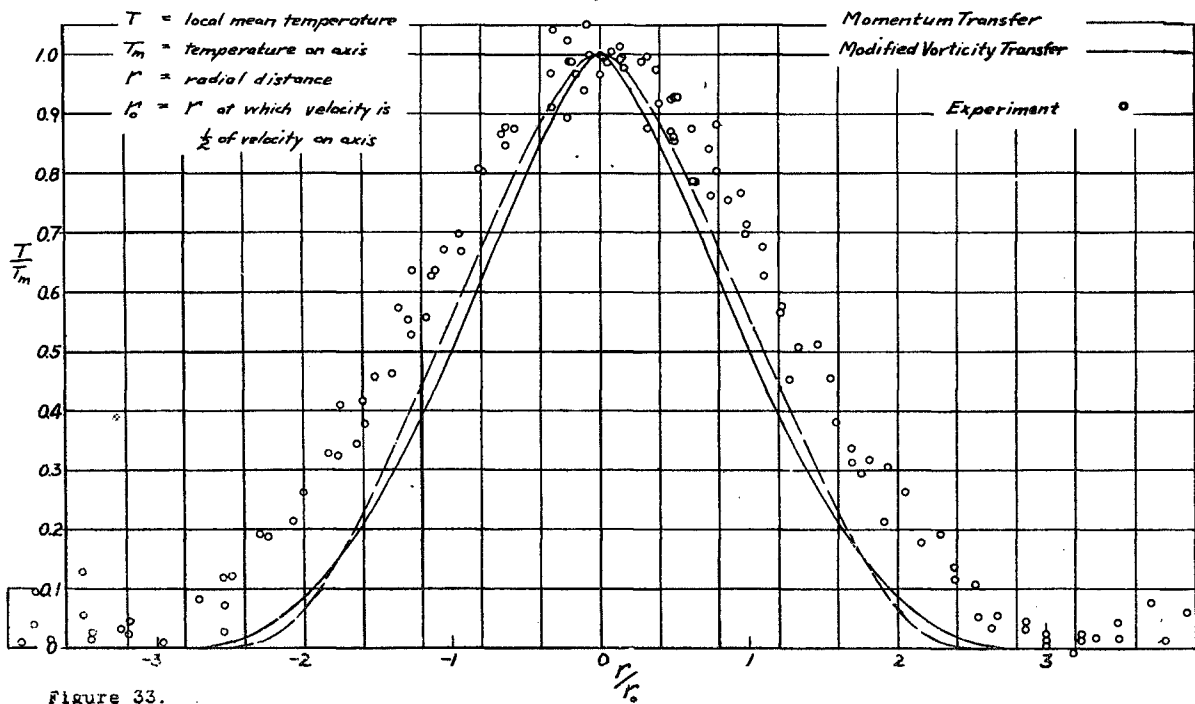
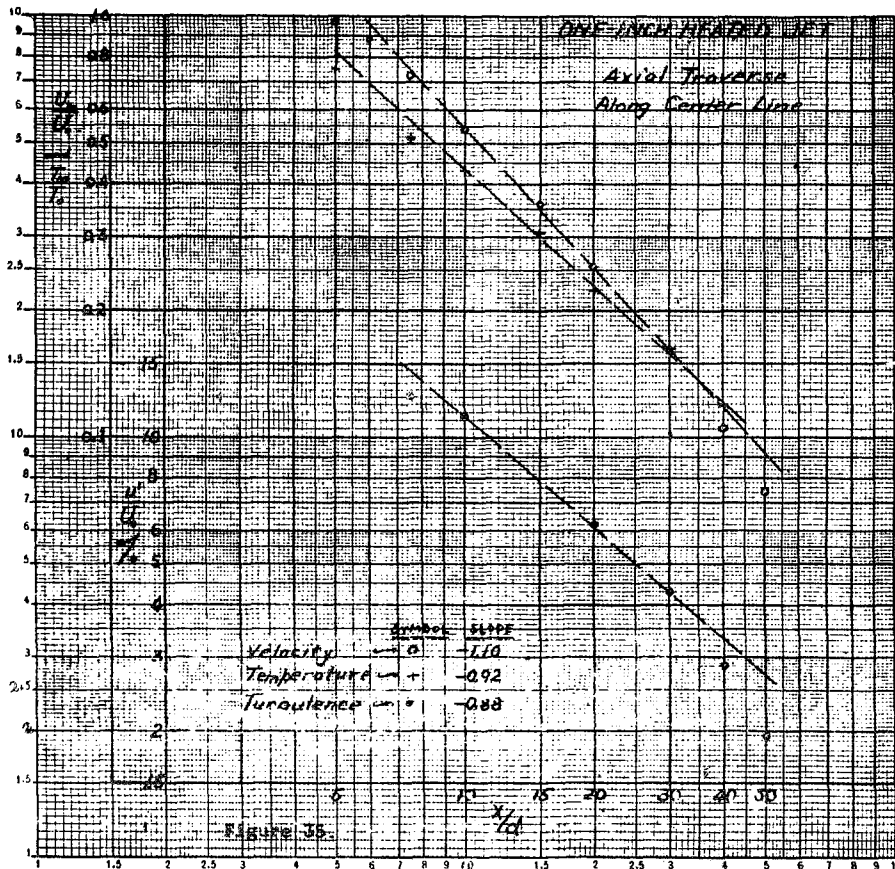
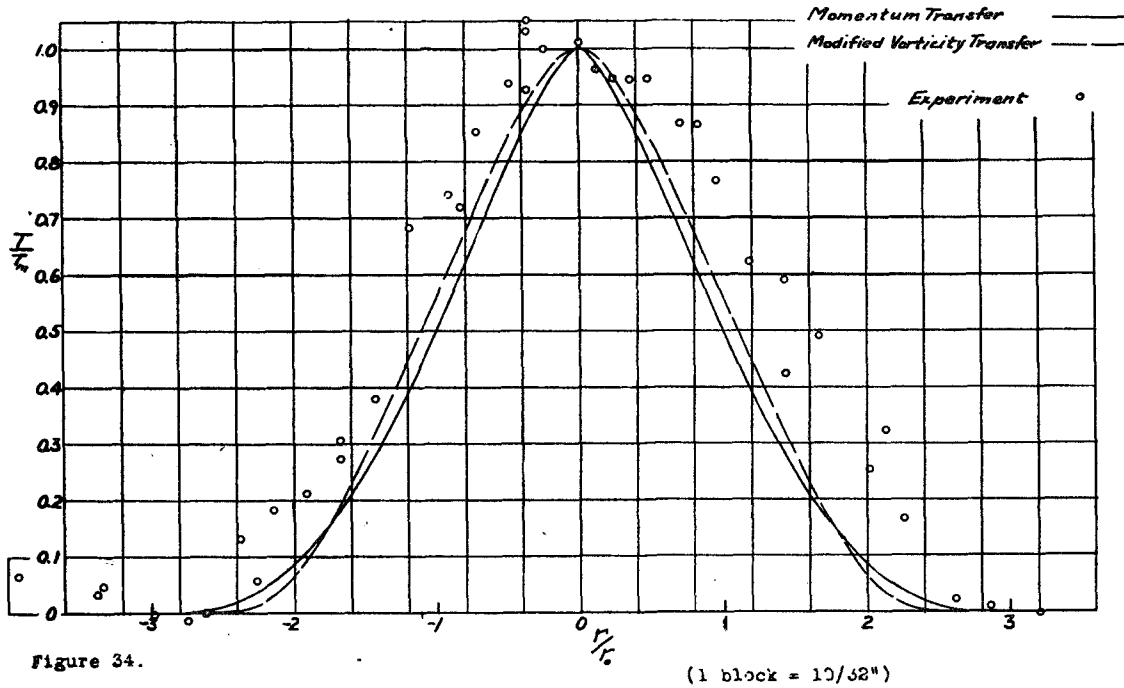


Figure 33.

ONE-INCH HEATED JET  
Lateral Temperature Distribution Compared with Theory  
 $X = 40$  dia.



### ONE-INCH HEATED JET Spread of Mean Velocity and Temperature

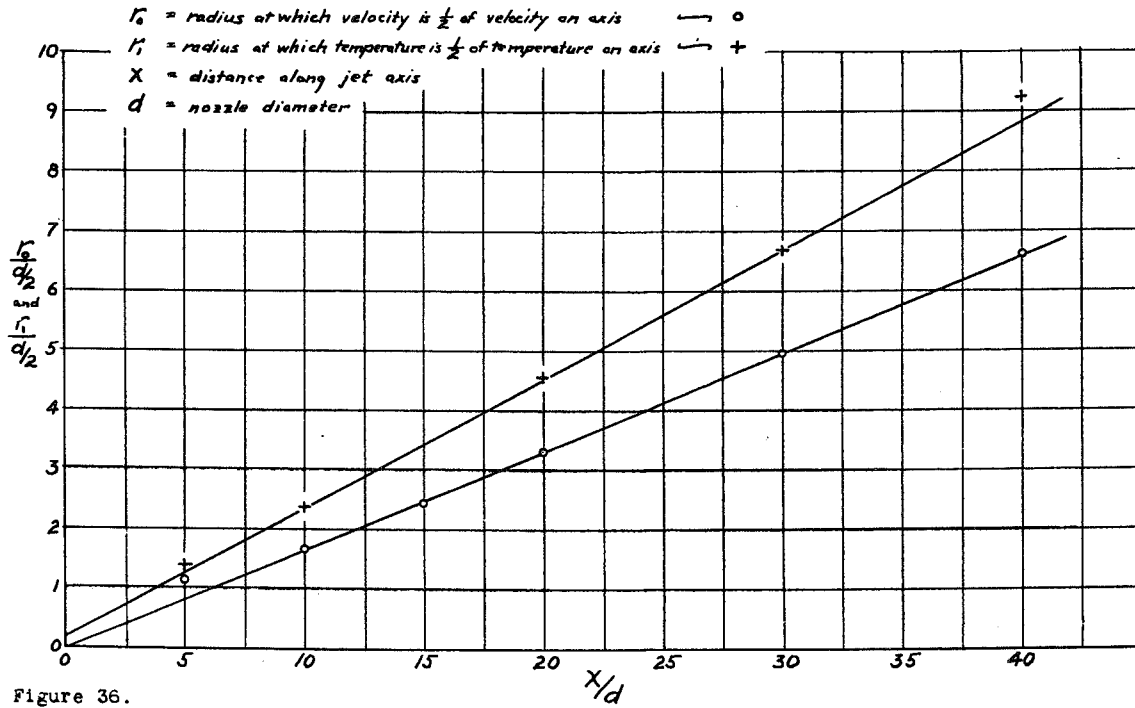


Figure 36.

(1 block = 10/32")

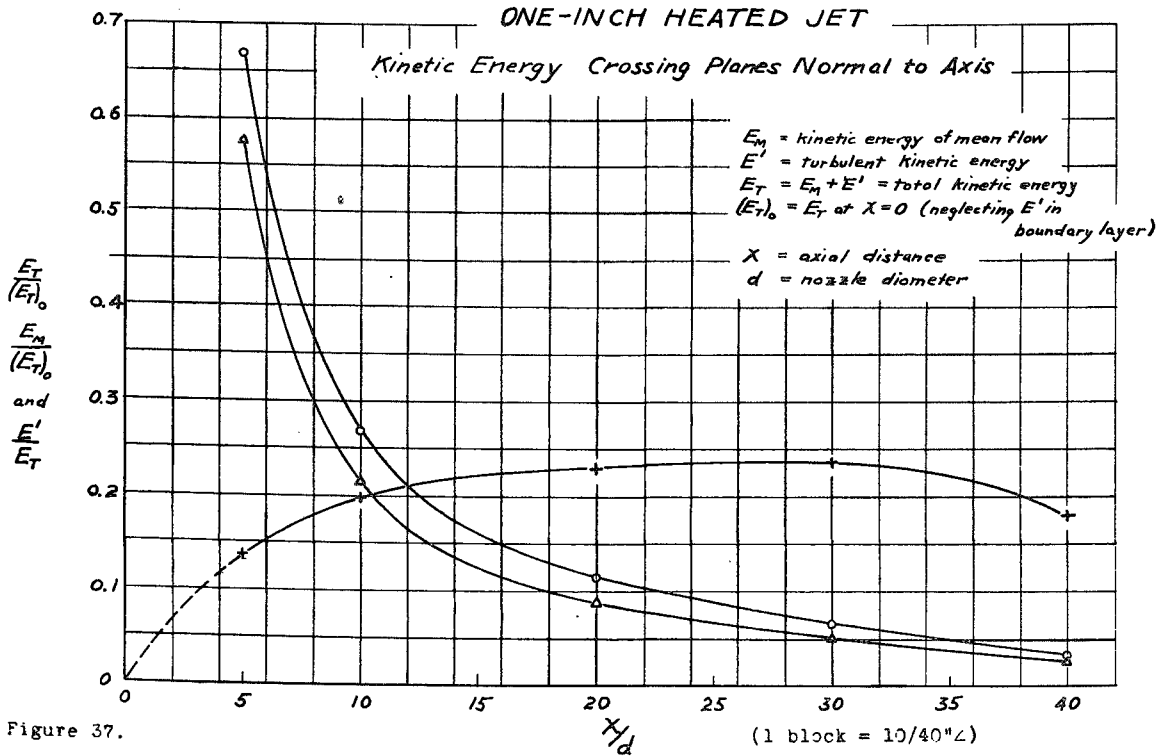


Figure 37.

(1 block = 10/40"Δ)

ONE-INCH HEATED JET  
Ratio of Turbulent Shear to Laminar Shear  
 $X = 20$  dia.

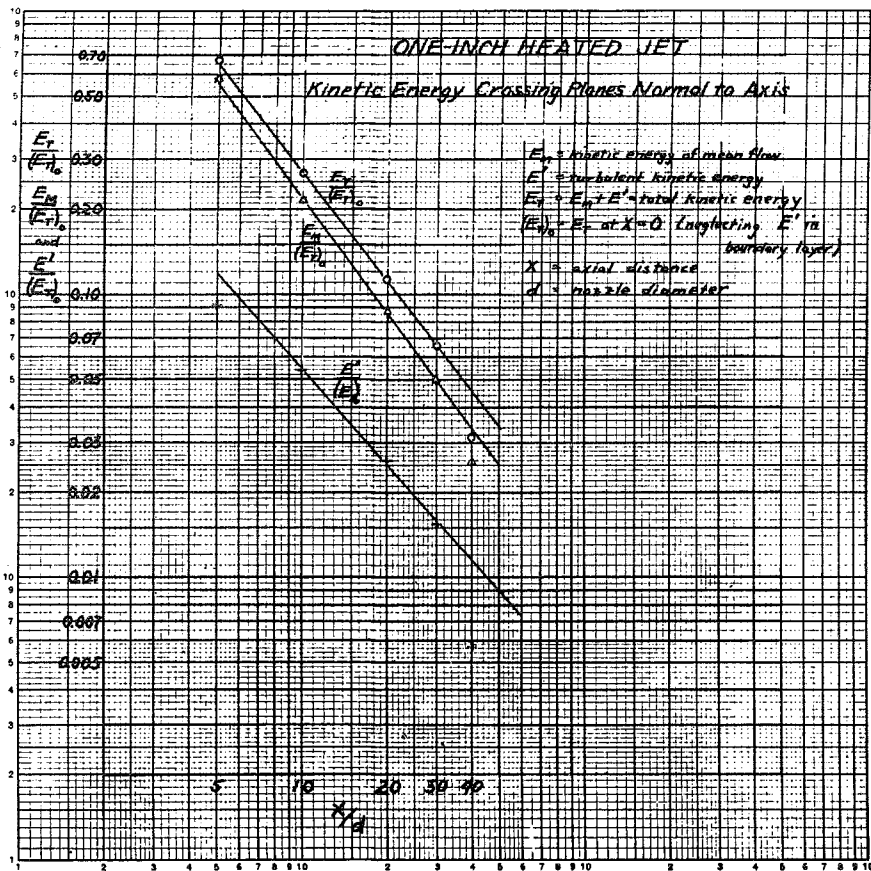


Figure 38.

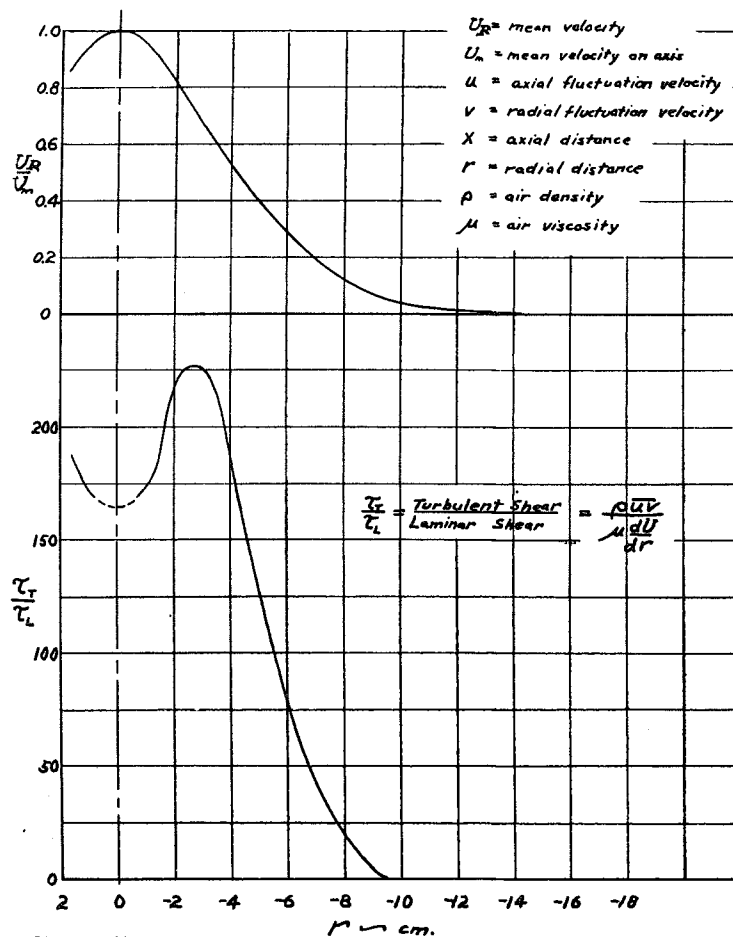


Figure 39.

(1 block =  $10/32''$ )

ONE-INCH HEATED JET

Comparison Between Total Shear Computed from Velocity Profile  
and Measured Turbulent shear

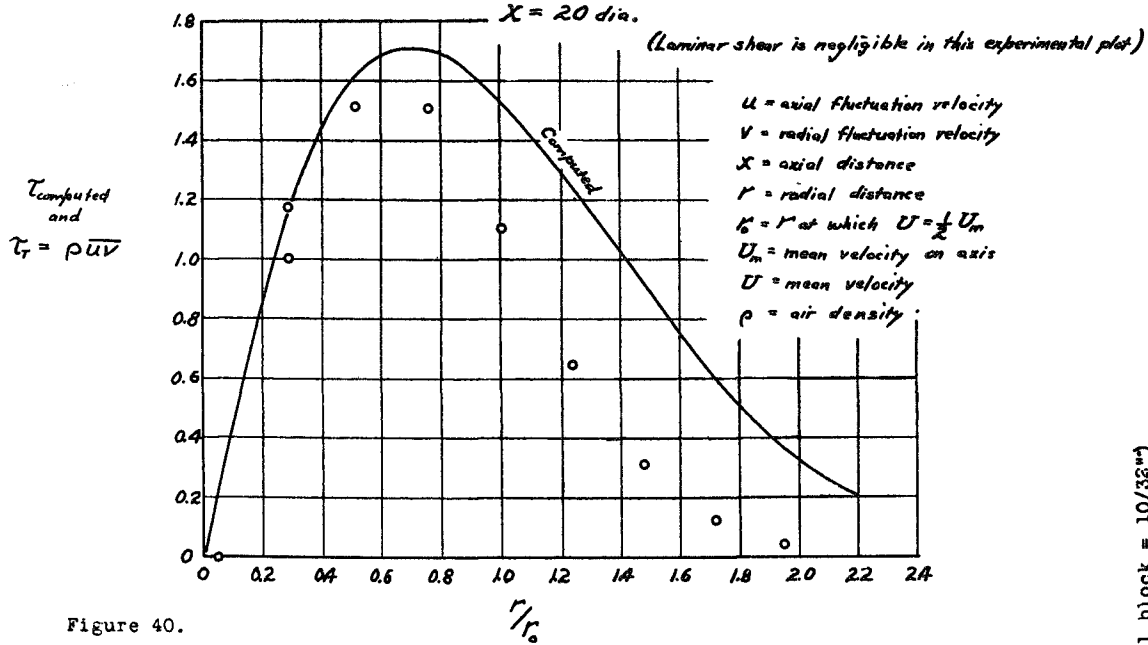


Figure 40.

(1 block = 10/32")

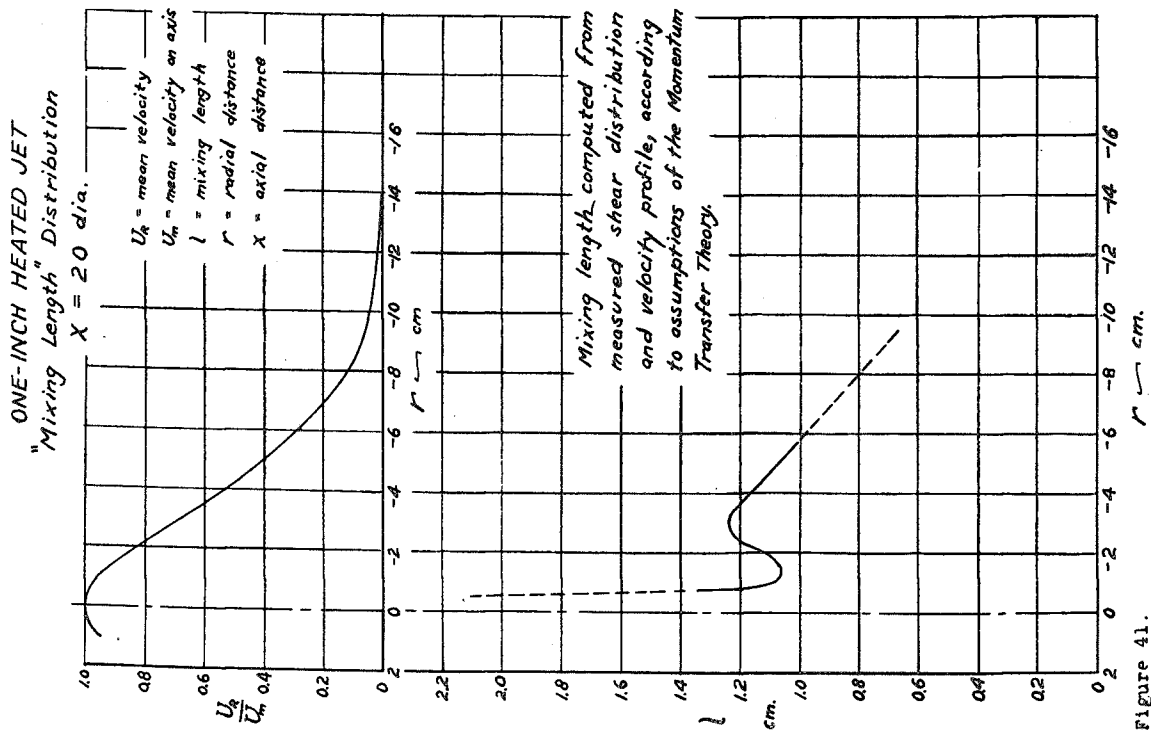


Figure 41.

HOT-WIRE ANEMOMETER

Correction to Measured Mean Velocity  
for Effect of Turbulence

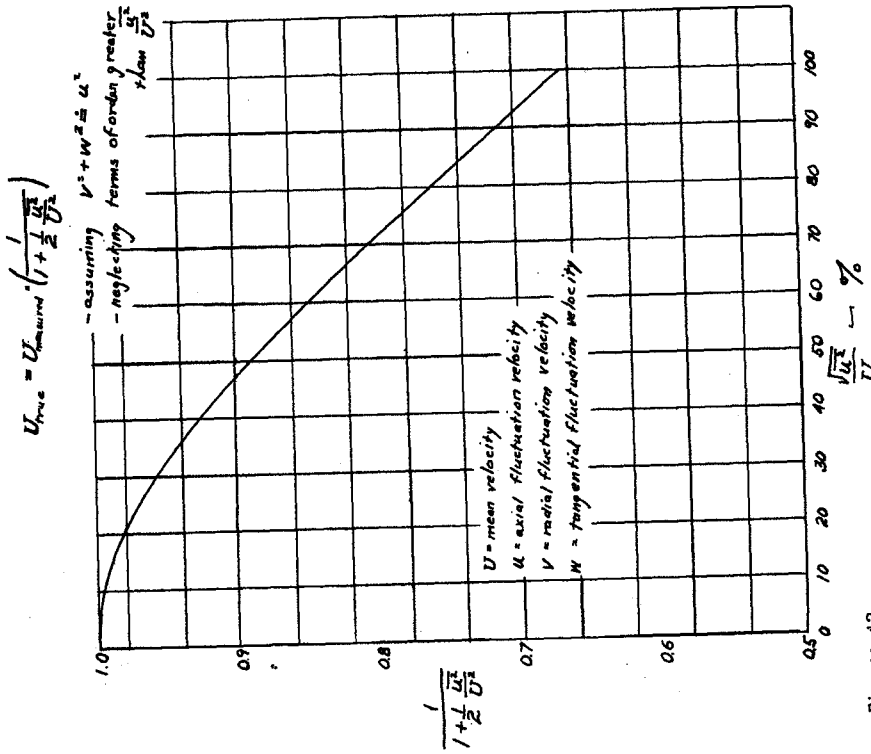


Figure 42.

GALCIT HOT-WIRE VIBRATOR  
Test of Hot-wire Response to High Turbulence Levels

$\frac{u}{U}$  = turbulence level

SYMBOL VELOCITY  
 ○ 2 meters/sec approx.  
 □ 5 " "  
 • 12 " "

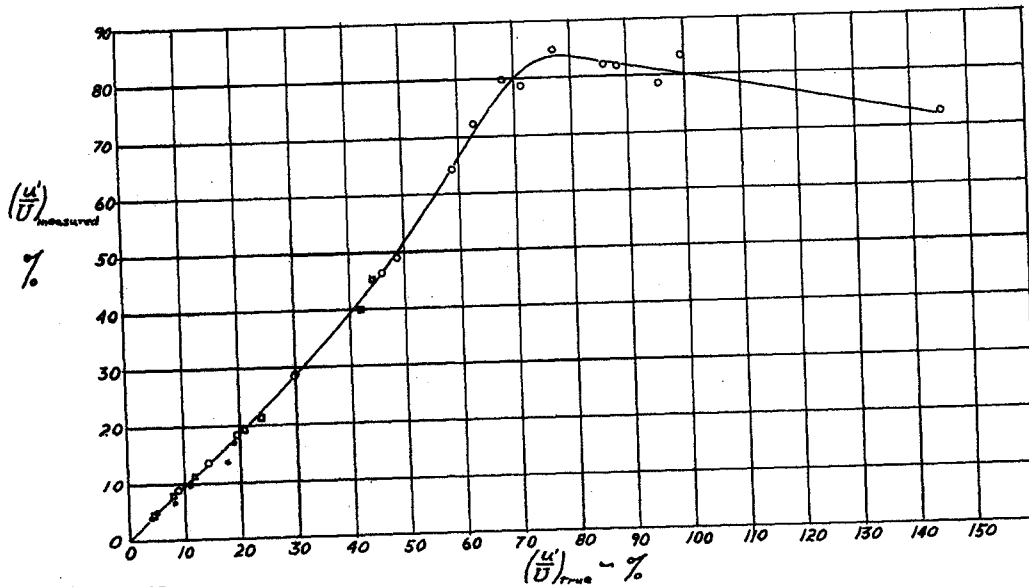


Figure 43.

(1 block = 10/32")

FORM 3 (13 OCT 47)  
Corrsin, Stanley

DIVISION: Power Plants, Jet and Turbine (5)  
SECTION: Performance (16)  
CROSS REFERENCES: Engines, Jet propulsion - Testing  
(33700); Flow through ducts (41200); Thermal  
measurement (93500)

ATI- 7835

ORIG. AGENCY NUMBER  
ACR-3123

REVISION

AUTHOR(S)

AMER. TITLE: Investigation of flow in an axially symmetrical heated jet of air

FORG'N. TITLE:

ORIGINATING AGENCY: National Advisory Committee for Aeronautics, Washington, D. C.

TRANSLATION:

COUNTRY	LANGUAGE	FORG'N CLASS	U. S. CLASS.	DATE	PAGES	ILLUS.	FEATURES
U. S.	Eng.		Unclas.	Dec '43	55	43	photos, diagrams, graph

#### ABSTRACT

Determination of suitable aerodynamic setup was primary purpose of test but, when final flow arrangement was achieved, attention was turned to measuring equipment. Result was construction of four-wire, two-amplifier, hot wire set. Preliminary tests showed serious asymmetry at low axial distances; change to smaller jet size was indicated. It is found that either velocity or temperature distribution can be made to give fairly good check between theory and experiment in turbulent jet cone, but never both velocity and temperature simultaneously.

NOTE: Requests for copies of this report must be addressed to: N.A.C.A.,  
Washington, D. C.

T-2, HQ., AIR MATERIEL COMMAND

AIR TECHNICAL INDEX

WRIGHT FIELD, OHIO, USAAF

WF-O-21 (MAR 47)